triosis, adenomyosis, uterine fibroids, pelvic inflammatory disease, menstruation, and benign cysts [6–9]. In addition, it has been demonstrated that the serum CA-125 level may decrease in CCA. Meyer and Rustin [10] previously reported that 50% of patients with CCA did not show abnormal CA-125 levels. Thus CA-125 measurements cannot often contribute to detection of the ovarian cancer in the clinic, and this failure may lead to difficulties in providing a proper therapy. Consequently, to achieve a more successful clinical treatment of ovarian cancer, new markers are needed that improve specificity and early detection of particular malignant types.

Recent advances in analytical technology for proteins offer exciting opportunities for finding novel biomarkers. Today, two major strategies are mainly used to discover clinically useful candidates by a proteomic approach. One of them utilizes a SELDI-TOF system [11–13], and the other is a method based on 2-D PAGE coupled with MS. Especially the SELDI-TOF, which generates the protein patterns by MS, has reportedly been used to find some biomarkers that are thought to have powerful potentials for application to diagnostic tests instead of CA-125 [14–20]. However, the targets are limited to small molecules (<20 kDa), and almost all of the protein peaks detected by this system are not easily identified as protein molecules. Thus, the findings cannot provide any information about the relationships and the roles of the marked proteins to the underlying pathology. On the other hand, the 2-D PAGE-based method targets the proteins appearing in a wide range of molecular weights, from 10 kDa to over 100 kDa. A 2-D image obtained from a biological sample gives a lot of information about proteins, which include expression volumes, actual *p*Is and molecular weights. The exclusive software for 2-D imaging assists in differential analysis of the protein spots separated in multiple 2-D images with good accuracy. Continuous analysis using MS provides additional information about protein identification and modification. Consequently, several reports have described new biomarkers for ovarian cancer by using this 2-D-based method [21, 22].

The aim of the present study was to identify proteins expressed characteristically in the malignant ovarian cancer, CCA, by using the proteomic procedure. It is hoped that some of the characteristically expressed proteins in CCA can serve as new diagnostic markers for CCA. In addition, if these proteins play major roles in progression of ovarian cancer to a malignant type, they may be candidates for therapeutic target molecules. To find these proteins, our previously established two ovarian cancer cell lines termed OVISE and OVTOKO were used. Both cell lines were derived from human epithelial ovarian CCA, and they have conserved the representative CCA malignant characteristics such as highly infiltrative growth and metastasis after transplantation to mice [23]. The analysis was performed using a 2-D PAGE-based method, which is a fluorescent 2-D differential gel electrophoresis (2-D DIGE). The 2-D DIGE differential analysis was performed using the DeCyder software [24]. Selected proteins were identified by MS, and we further preliminarily confirmed the expression of identified proteins in extirpated tissue obtained from a patient with CCA.

2 Materials and methods

2.1 Materials

CyDye DIGE Fluors (Cy2, Cy3, and Cy5 for minimal labeling), Pharmalytes (pH 3–10), Immobiline DryStrip (pH 3–10 NL), TEMED, Bind-Silane, DMF, SDS, acrylamide, and *N,N*-methylenebisacrylamide were purchased from Amersham Biosciences (Uppsala, Sweden). Urea was from ICN Biomedicals (Aurora, OH, USA). Other chemicals were obtained from Wako Pure Chemical Industries (Osaka, Japan). Protease inhibitor mixture cocktail (Complete, EDTA-free) was from Roche Diagnostics (Mannheim, Germany). Modified trypsin sequence grade was from Promega (Madison, WI, USA), and the SYPRO Ruby gel staining kit was purchased from BioRad (Hemel Hempstead, UK).

2.2 Culture cells and tissues

Three human gynecological cancer cell lines were analyzed in this experiment: MCAS, established from ovarian mucinous cystadenocarcinoma, was provided by the Japanese Cancer Research Bank (JCRB 0240), and cloned by the limiting dilution method. OVISE and OVTOKO were established from metastatic ovarian CCA [23, 25]. The cells were maintained in RPMI 1640 medium (Nissui Pharmaceuticals, Tokyo, Japan) supplemented with 10% fetal calf serum (FCS; JRH, Lenexa, KS) at 37°C in a humidified atmosphere of 5% CO_2 and 95% air. When the cells grew exponentially and reached semiconfluency in plastic culture dishes (90 mm diameter, Sumibe Medical, Tokyo, Japan), they were washed twice with PBS and harvested with a rubber policeman. The cells collected in 15 mL conical tubes (Sumibe Medical) were further washed three times with PBS and stored at −80°C until use.

Ovarian cancer tissues were taken from freshly isolated surgical resections in the operating room, rinsed thoroughly with saline, and snap-frozen within 5 min. The frozen tissues were stored at −80°C until use. In this proteomic study, two frozen tissues were analyzed. One was classified as mucinous cystadenoma and was derived from a 47-year-old patient. Another was classified as CCA and was derived from a 63-year-old patient with ovarian cancer, FIGO stage Ic. A documented informed consent was obtained from each patient, and the study was performed in accordance with the guidelines of the ethical committee of Yokohama City University School of Medicine.

2.3 Sample preparation for 2-D DIGE

Sample lysing buffer (30 mM Tris-HCl, 7 M urea, 2 M thiourea, 4% CHAPS, 1× Complete, EDTA-free protease inhibitor, and 1 mM EDTA-2Na, pH 8.5) was added to each tube containing frozen ovarian cancer culture cells. The volume of added lysing buffer was fixed at 50 μL *per* 1.0×10^6 cells. Then the tube was vortexed vigorously for a few minutes until all cells were completely lysed, and the suspensions were centrifuged at $15\,000 \times g$ for 1 min at 4°C. The separated supernatants were centrifuged for an additional $15\,000 \times g$ for 5 min at 4°C, before being used for 2-D DIGE samples. Protein extracts from cancer tissues were prepared by the same method after the tissues obtained surgically were crosscut with surgical scissors and scalpels to a homogenous suspension. Total protein concentrations were determined by Protein Assay kit purchased from BioRad using bovine plasma gamma globulin as a standard.

Each protein sample was labeled with 400 pmol of Cy3 or Cy5 *per* 50 μg of protein according to the manufacturer's protocol (Amersham Biosciences). As the internal control for 2-D DIGE, protein sample mixture that contained equal amounts of samples for analysis were labeled with Cy2 as well as Cy3 and Cy5. After labeling, 50 μg of Cy2-, Cy3-, and Cy5-labeled protein samples to be separated in the same 2-D gel were mixed in practical combinations for 2-D DIGE analysis [26].

2.4 2-D DIGE analysis

A schematic outline of 2-D DIGE is described in Fig. 1A. Prior to IEF, an equal volume of 2× sample buffer (7 M urea, 2 M thiourea, 4% CHAPS, 2% DTT, and 2% Pharmalytes with a pH of 3–10) was added to the labeled sample mixture and incubated on ice for 10 min, then rehydration buffer (8 M urea, 4% CHAPS, 2% DTT, 1% Pharmalytes with a pH of 3–10 and a grain of Bromophenol blue) was added, resulting in a final volume of 450 μL. IEF was carried out in Immobiline DryStrip (pH 3–10 NL, 24 cm) and performed on an IPGphor (Amersham Biosciences). After rehydration of the IPG strips with the labeled samples and rehydration buffer for 12 h at 20°C, focusing was carried out at 500 and 1000 V for 1 h each and 6000 V for a total of 90 KV·h. The current was limited to 50 μA *per* strip. Prior to SDS-PAGE, each strip was equilibrated with 10 mL of equilibration buffer A (50 mM Tris-HCl, 6 M urea, 2% SDS, 30% glycerol, and 0.5% DTT, pH 8.8) for 15 min with gentle shaking, followed by 10 mL of equilibration buffer B (50 mM Tris-HCl, 6 M urea, 2% SDS, 30% glycerol, 4.5% iodoaceta-

A

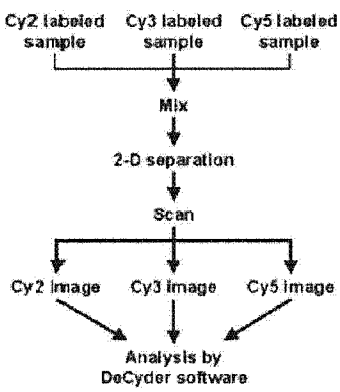

B

Gel	Cy2	Cy3	Cy5
No.1	I.C.	MCAS	MCAS
No.2	I.C.	OVISE	OVISE
No.3	I.C.	OVTOKO	OVTOKO
No.4	I.C.	MCAS	OVISE
No.5	I.C.	OVISE	OVTOKO
No.6	I.C.	OVTOKO	MCAS

C

Gel	Cy2	Cy3	Cy5
No.1	I.C.	Mixture of three cell line samples	Protein extract from tissue A
No.2	I.C.	Mixture of three cell line samples	Protein extract from tissue B
⋮	⋮	⋮	⋮

Figure 1. Methods for proteome analysis by 2-D DIGE. (A) Schematic outline of 2-D DIGE. The mixture of the separately labeled samples was separated in one 2-D gel. The gel images were scanned for Cy-dyes independently and analyzed by DeCyder software. (B) Experimental design for 2-D DIGE analysis of patients from three cell lines. The mixture of three samples labeled by Cy2 was used as the internal control (I.C.) and the Cy2 image of gel no. 1 was designated as "master image." (C) Experimental design for 2-D DIGE analysis comparing the spots of tissue samples with those of cell lines. The mixture of three cell line samples (that was the same sample as I.C. in "B") was labeled by Cy3, and a protein sample prepared from each tissue specimen was labeled by Cy5. These labeled proteins were run together with the Cy2-labeled proteins containing the mixed-sample of three cell lines and tissue samples on each gel as the I.C. for quantification analysis.

mide, and a grain of Bromophenol blue, pH 8.8) for a further 15 min. The IPG strips were then loaded and run on 12.5% polyacrylamide Laemmli gels [27] using the Ettan DALT Twelve apparatus (Amersham Biosciences). The Laemmli gels for second-dimension electrophoresis were cast previously in 21 × 24 cm^2 glass plates, of which one inner side was precoated with Bind-Silane. Gels were run at 1 W *per* gel constant power at 20°C until the front of the Bromophenol blue dye reached the bottom of the gels.

Gel images were collected using the Typhoon 9400 (Amersham Biosciences) fluorescence gel scanner. The Cy2-labeled gel images were collected using a 488 nm laser as excitation source and an emission filter of 520 nm BP (band pass) 40. The Cy3-labeled gel images were collected using a 532 nm laser as excitation source and an emission filter of 580 nm BP30. The Cy5-labeled gel images were collected using a 633 nm laser as excitation source and an emission filter of 670 nm BP30. After imaging for Cy-dye components, the nonsilanized glass plates were removed and stained with SYPRO Ruby by using the staining kit according to the manufacturer's protocol. The stained images were acquired using a 457 nm laser as excitation and an emission filter of 610 nm BP30. All these Cy-dye and SYPRO Ruby images were scanned at 100 μm resolution. Cy-dye images were cropped to remove extra areas by ImageQuant software version 5.2 (Amersham Biosciences), and then imported into DeCyder software version 5.02 (Amersham Biosciences).

Expressed proteins, seen as spots in-gel images, were detected with the DIA (differential in-gel analysis) module of DeCyder software. These images were normalized and statistically analyzed to identify and quantify differentially expressed proteins with this DIA module. The BVA (biological variation analysis) module of DeCyder was used to calculate average abundance changes and analyze the differential expression of the proteins statistically across all gels. All normalized spot volumes and ratios data were exported from DeCyder software, and the contribution from each analyzed sample was calculated and assessed with Excel software (Microsoft).

2.5 Identification of proteins by MS

Protein spots of interest were excised from SYPRO Ruby stained 2-D DIGE gels, and in-gel digestion was performed as previously described [28, 29]. The gel pieces were washed three times with 60% ACN solution containing 100 mM NH_4HCO_3 and dried using an evaporator. The dried gel pieces were rehydrated with 100 mM NH_4HCO_3 containing 12.5 ng/μL of trypsin, and then incubated at 37°C for 16 h. After digestion, peptide fragments in the gel pieces were extracted with 60% ACN solution and evaporated to complete dryness, followed by resuspension in 20 μL of 0.1% formic acid and 0.01% TFA solution. The solutions filtered by Ultrafree-MC with 0.22 μm Durapore (Millipore, Bedford, MA, USA) were used as sample for ESI Q-TOF MS.

The samples containing purified peptide fragments were desalted using capillary LC nano-LC system (LC packing, Sunnyvale, CA, USA) equipped with a precolumn, PepMap C18 (320 μm id × 1 mm, LC packing), and applied continuously to an analytical column, MonoCap for Peptide (100 μm id × 250 mm, GL Science, Tokyo, Japan). The peptide fragments were eluted by gradient flow of ACN and distilled water containing 0.1% formic acid and 0.01% TFA, then injected directly into Q-TOF MS (Q-Tof micro, Micromass, Manchester, UK) through a nano-LC probe (ESI) under the following analytical conditions: cycle time, 2.10 s; scan duration, 2.00 s; retention window, 0.00–70.00; ionization mode, ES+; mass range, 400–1800 Da. Four parent masses were selected for MS/MS analysis with collision energy of 20–30 eV. Data acquisition was carried out using MassLynx version 3.5 (Micromass), and peptide sequence analysis was performed using BioLynx software (Micromass). The sequence information was submitted to ProteinLynx software (Micromass) and MASCOT programs (http://www.matrixscience.com/), and the results of identification by MS/MS analysis were scored. The top-scoring proteins with ProteinLynx score of more than 200, MASCOT score of more than 60 and judged by MASCOT to be more than "significant," were considered to be the corresponding proteins. In these searches for protein identification, Swiss-Prot and EMBL peptide databases were used.

3 Results

3.1 2-D DIGE analysis of proteins from culture cells

Protein profiles from three human ovarian cancer culture cells were analyzed by 2-D DIGE. The experimental design for this proteomic analysis was shown in Fig. 1B. In order to analyze and compare the expressed protein amounts statistically among three cell lines, the 2-D DIGE was designed to capture four fluorescent scan images in each cell line that were composed of two Cy3- and two Cy5-images. Additionally, the experiment was designed to capture two different Cy-dye-labeled images derived from a single gel scanning of the same sample, which was carried out on gel numbers 1–3. These gel images, analyzed by DeCyder-DIA software, allowed us to confirm that there were no significant differences between spot patterns and volumes of Cy3- and Cy5-labeled proteins. Figure 2 shows the representative Cy5 imaged 2-D patterns of proteins extracted from each culture cell line as follows: (A) MCAS, (B) OVISE, (C) OVTOKO. We observed 2189 spots in a master gel (gel no. 1, Cy2) image, and between 2132 and 2536 spots in Cy3 and Cy5 gel images after applying 50 μg of Cy-dye-labeled proteins. The normalized and averaged volume data for all detected spots were generated from the protein expression profile of 2-D DIGE, calculated by DeCyder-BVA software, and depicted as scattergrams between the spot volumes of two ovarian cancer cell lines in Fig. 3. The plotted 870 spots in the presented scat-

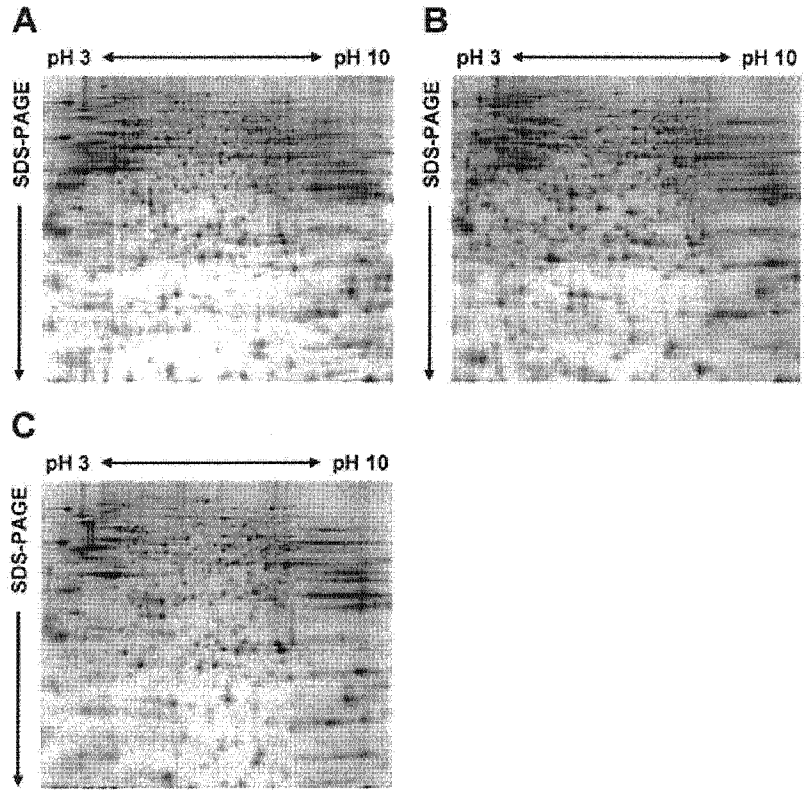

Figure 2. 2-D gel images of Cy5-labeled proteins (50 μg) extracted from human ovarian cancer culture cells. (A) MCAS, gel no. 1; (B) OVISE, gel no. 2; (C) OVTOKO, gel no. 3. IEF as the first dimension separation was over a non-linear pH range of 3.0–10.0. The second dimension separation was carried out by SDS-PAGE in a 12.5% polyacrylamide gel.

tergrams were only included proteins that were clearly detected in all gel images (obscure spots were not included in the scatter analysis). The scatter analysis revealed that there was no noticeable difference in the distribution patterns of spot volumes between the mucinous adenocarcinoma cell lines, MCAS and CCA, OVISE and OVTOKO (correlation coefficient; $r = 0.870$ and 0.850, respectively) or between the two CCA cell lines ($r = 0.869$). However, observing the respective spot volumes, remarkable changes in some protein expressions were found in all scattergrams, which demonstrated the existence of proteins with quantitative changes depending on each cell line character. To focus on these proteins, the individual spots whose volumes were increased or decreased in the respective cell lines, according to the spot lists in the DeCyder software, were extracted and analyzed. The spots showing two-fold volume differences are summarized in Fig. 4, including 447 spots that had volumes with intensities that were higher than the 2.5×10^5 average fluorescent intensity calculated by the DeCyder software. From this distribution analysis, it appeared that 18 expressed proteins were up-regulated in both CCA cell lines, OVISE and OVTOKO, and 31 proteins were down-regulated as compared with those in the mucinous adenocarcinoma cell line, MCAS. These characteristic spots in the CCA cell lines were marked in Fig. 5 on the master image of gel no. 1 Cy2.

3.2 Identification of characteristically expressed proteins in CCA

Characteristically expressed proteins in the CCA cell lines, OVISE and OVTOKO, as compared with the mucinous adenocarcinoma cell line, MCAS, were analyzed by ESI Q-TOF MS to determine their amino acid sequences, which were then submitted to the Swiss-Prot and EMBL peptide databases for protein identification. The spots of interest were cut out from a SYPRO Ruby stained 2-D DIGE gel, subjected to in-gel digestion and analyzed to identify proteins. Out of 18 up-regulated and 31 down-regulated spots in OVISE and OVTOKO, 13 up-regulated and 11 down-regulated spots were identified. In addition, up- or down-regulated spots that indicated at least two-fold differences in either OVISE or OVTOKO in comparison with MCAS were identified. All analyzed spots were well separated from other spots in 2-D gel, therefore the second and/or other candidates could not be identified by the MS data search. The results of the protein identifications are shown in Table 1, together with the respective UniProt accession numbers, spot volume ratios (CCA cell lines *vs.* mucinous adenocarcinoma cell line), and protein functions, except for the nuclear matrix protein NMP200, which was an unknown protein.

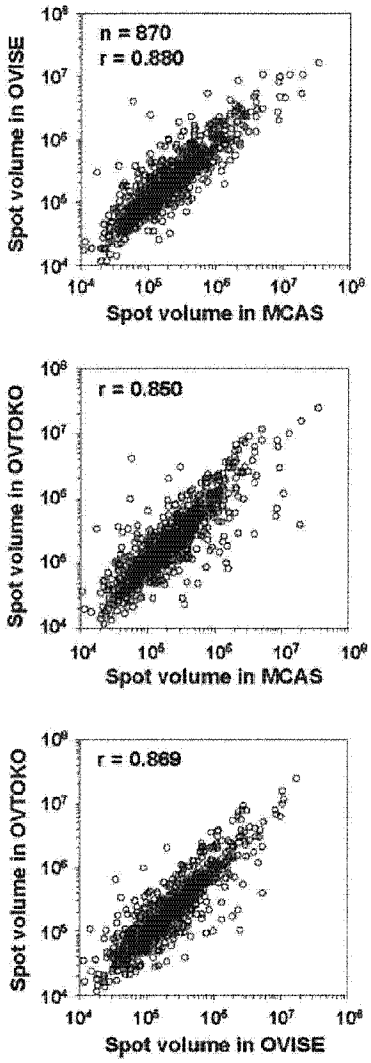

Figure 3. Scattergrams of spot volumes detected in 2-D gels of two human ovarian cancer culture cells. Eight hundred and seventy spot volume data were generated from protein expression profiles of 2-D DIGE data. The spots were normalized by each matched spot in the master image, which was used as the internal control image in each 2-D gel, and averaged.

3.3 Expression of addressed proteins in cancer tissue

We examined whether the differentially changed proteins in the CCA cell lines were also expressed in surgically excised specimens obtained from a patient with CCA. This examination was also carried out using the 2-D DIGE system. The experimental design was shown in Fig. 1C. In this analysis, a Cy5-labeled sample was the protein extract prepared from extirpated tissues of CCA and mucinous cystadenoma. The profile of the Cy5-labeled tissue proteins was compared in one 2-D DIGE run with the profile of the Cy3-labeled pro-

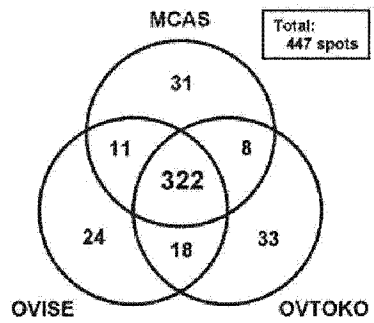

Figure 4. Distribution of the spots showing more than two-fold volume differences from the other human ovarian cancer culture cell lines, as detected by 2-D DIGE. A total of 447 analyzed spots had volumes that showed a higher fluorescent intensity than the average 2.5×10^5 intensity calculated by the DeCyder software.

teins from the three cultured cell lines. A mixture of Cy2-labeled proteins containing equal amounts of all analytical samples was used as an internal control. After 2-D separation, the fluorescent images were collected, and the detected spots of the tissue samples in Cy5-images were compared with those of the human ovarian cancer cell lines in Cy3-image to identify the addresses. The merged image made clear whether a detected spot in Cy3- and Cy5-image was derived from an equivalent protein or not. The significant spots in 2-D gels from tissue samples were additionally identified using MS, and confirmed the identified proteins that were identical proteins resulting from the analysis of the cell samples. Subsequently, each spot volume was analyzed by DeCyder software using the Cy2 image as internal control. The representative 2-D image of Cy5-labeled extract sample prepared from a CCA tissue was shown in Fig. 6.

In the 2-D analysis, we observed some high-abundant serum proteins (*e.g.*, serum albumin, transferrin, antitrypsin, and apolipoprotein A-I) in the images of tissue samples that originated from contamination of the tissue with blood (Fig. 6). The rates of these extra proteins were different from the samples that were responsible for the states of original extirpated tissues and preparations of samples. Consequently, these contaminated proteins reduced the variation in intensity of spots that were derived from proteins that were characteristic of the cancer tissue. However, using the reference profile of spots that were of interest in CCA cells on 2-D gel, it was possible to analyze the changing volumes of these proteins in the cancer tissue specimens. In this study, 13 of the 18 up-regulated and 8 of the 31 down-regulated proteins in the CCA culture cells were observed clearly in 2-D gel images collected from both CCA and mucinous cystadenoma tissues. In these spots, 7 of the 13 (54%) up-regulated proteins were increased and 3 of the 8 (38%) down-regulated proteins were decreased at least 1.2-fold with statistically significance by Student's *t*-test ($p<0.05$), respectively, in CCA tissue in comparison with the mucinous adenoma tissue. Differential highly expressed proteins in CCA tissue are

Table 1. Differentially expressed proteins in human ovarian cancer cells

Spot no.	Protein name	Accession no.	Volume ratio (OVI/MC)	Protein (OVT/MC)	Function
Up-regulation (more than two-fold)					
OVISE, OVTOKO>MCAS					
582	Elongation factor 2	P13639	2.8	2.9	Protein biosynthesis
794	Glycyl-tRNA synthetase	P41250	2.2	2.0	tRNA modification
953	T-plastin	P13797	2.9	3.2	Actin-binding protein
1237	Glutamate carboxypeptidase-like protein 1	Q96KP4	2.1	2.3	Peptidase
1402	Alpha enolase	P06733	2.2	2.3	Glycolysis
1712	Apolipoprotein L2	Q9BQE5	2.0	5.3	Lipid binding protein
1722	Transaldolase	P37837	5.1	4.9	Glycolysis
1752	L-lactate dehydrogenase B chain	P07195	67.9	69.9	Glycolysis
1839	Annexin A4	P09525	3.6	9.9	Phospholipid-binding protein
1940	Phosphoglycerate mutase 1	P18669	4.9	3.8	Glycolysis
1987	Triosephosphate isomerase	P00938	3.2	3.0	Glycolysis
2041	GST P	P09211	7.1	2.8	Protein modification
2047	Peroxiredoxin 1	Q06830	4.1	3.2	Redox
OVISE>MCAS, OVTOKO					
581	Elongation factor 2	P13639	2.0	1.9	Protein biosynthesis
1184	Tryptophanyl-tRNA synthetase	P23381	3.1	1.4	Protein biosynthesis
1211	Glutamate dehydrogenase 1	P00367	2.1	1.4	Amino acid dehydration
1451	Adenosylhomocysteinase	P23526	2.5	1.3	Methyl transferase inhibitor
1479	Isocitrate dehydrogenase	O75874	5.5	−1.9	Glycolysis
1574	Macrophage capping protein	P40121	4.2	−1.9	Actin-binding protein
1836	Annexin A4	P09525	22.3	−1.1	Phospholipid-binding protein
1845	Delta3,5-delta2,4-dienoyl-CoA isomerase	Q13011	3.9	−2.2	Fatty acid oxidation cycle
1849	Purine nucleoside phosphorylase	P00491	2.2	1.0	Nucleotide synthesis
1944	Prohibitin	P35232	5.3	1.7	DNA synthesis inhibitor
1980	Heat shock 27 kDa protein	P04792	5.4	−1.6	Stress response
1997	Ran-specific GTPase-activating protein	P43487	3.2	1.4	Signaling transduction
2171	Cystatin B	P04080	6.5	−1.7	Thiol protease inhibitor
OVTOKO>MCAS, OVISE					
1117	Thioredoxin reductase	Q16881	1.0	3.4	Redox
1136	Nuclear matrix protein NMP200	Q9UMS4	1.0	9.9	(Unknown)
1573	Macrophage capping protein	P40121	1.9	3.2	Actin and DNA interaction
1775	L-lactate dehydrogenase A chain	P00338	−1.1	2.7	Glycolysis
1958	Phosphoglycerate mutase 1	P18669	−1.8	2.2	Glycolysis
1991	Triosephosphate isomerase	P00938	1.0	3.0	Glycolysis
2003	Ubiquitin carboxyl-terminal hydrolase isozyme L1	P09936	1.6	17.9	Ubiquitin processing
2119	Nucleoside diphosphate kinase B	P22392	1.7	2.0	Nucleotide synthesis
Down-regulation (more than two-fold)					
OVISE, OVTOKO<MCAS					
584	Elongation factor 2	P13639	−3.2	−2.8	Protein biosynthesis
1252	Cytokeratin 8	P05787	−2.3	−9.1	Cytoskeletal protein
1271	Cytokeratin 7	P08729	−3.4	−47.2	Cytoskeletal protein
1293	Cytokeratin 8	P05787	−3.6	−8.6	Cytoskeletal protein
1436	Cytokeratin 18	P05783	−3.1	−15.3	Cytoskeletal protein
1438	Ornithine aminotransferase,	P04181	−7.1	−5.1	Amino acid metabolism
1527	Cytokeratin 19	P08727	−3.5	−19.6	Cytoskeletal protein
1531	Cytokeratin 19	P08727	−4.2	−12.0	Cytoskeletal protein
1804	Annexin A3	P12429	−2.5	−2.2	Phospholipid-binding protein
1899	ER protein 29	P30040	−2.1	−2.7	Secretory protein processing
1956	Enoyl-CoA hydratase 1	P30084	−2.4	−2.6	Fatty acid oxidation cycle

Some protein spots expressed differentially in CCA cell lines were identified using ESI Q TOF-MS and listed with their UniProt accession numbers. The volume ratios were calculated from each spot volume generated from the protein expression profile of 2-D DIGE data by DeCyder-BVA. OVI, OVISE; MC, MCAS; OVT, and OVTOKO.

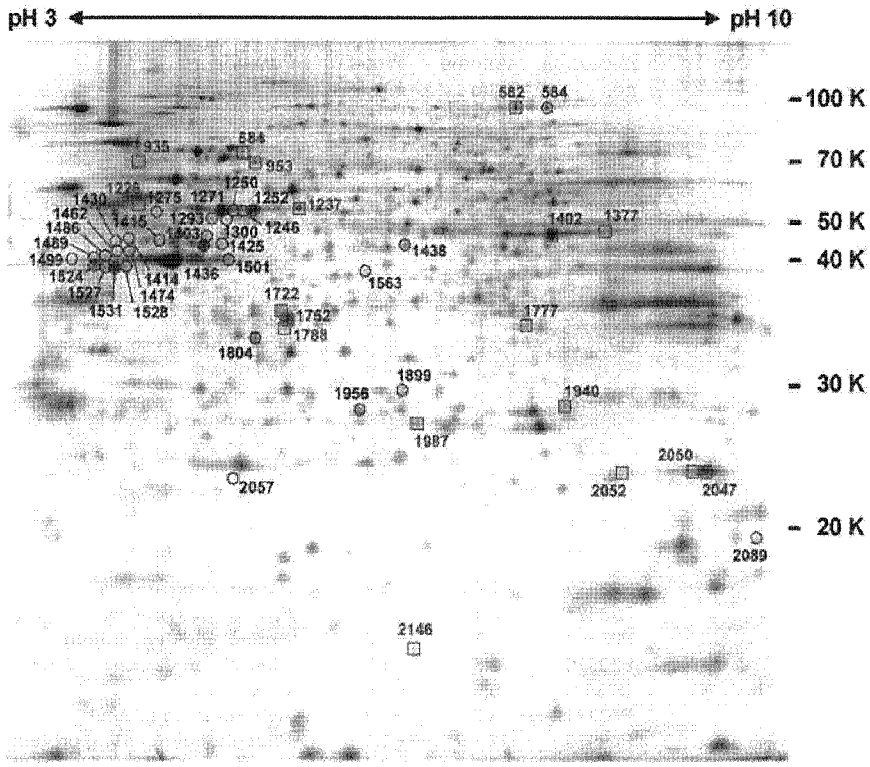

Figure 5. 2-D DIGE gel image of a Cy2-labeled mixed-sample as internal control (gel no. 1, master image). The marked spots were proteins that showed more than two-fold volume changes in comparison with MCAS in both OVISE and OVTOKO. Proteins that were induced were indicated by red squares ($n = 18$), those that decreased in volume by blue circles ($n = 31$).

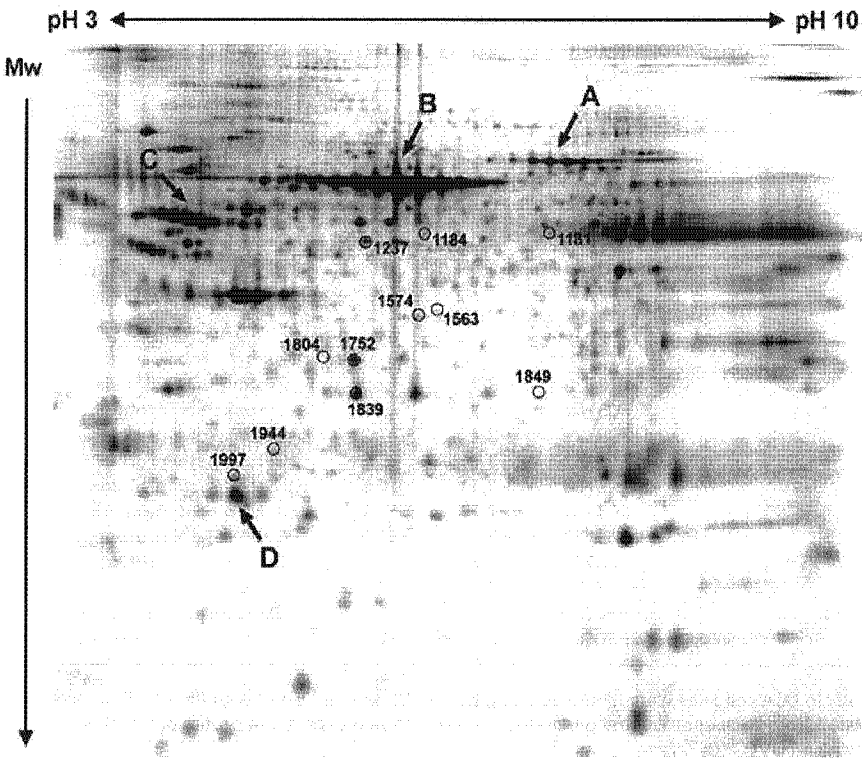

Figure 6. 2-D DIGE gel image of a Cy5-labeled sample prepared from a CCA tissue. The spots derived from the contaminated serum proteins were marked as follows: (A) transferrin; (B) albumin; (C) α-1 antitrypsin; and (D) apolipoprotein A-I. Additionally, the spots differentially expressed in tissue samples shown in Table 2 are indicated.

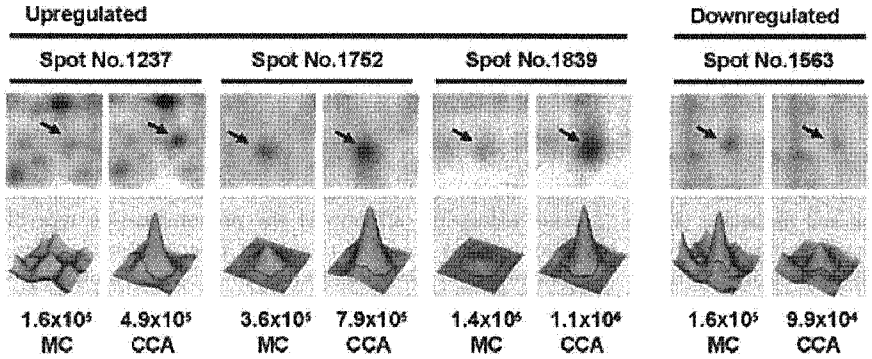

Figure 7. 3-D presentation of up- and down-regulated protein spots of human ovarian cancer tissue, mucinous cystadenoma (MC) and CCA. Cy5-labeled proteins extracted from human ovarian cancer tissues were separated in 2-D gels together with Cy3-labeled proteins prepared from culture cells of human ovarian cancer and Cy2-labeled protein mixture as the internal control. The marked spots in Fig. 5 were found in Cy3 images and also identified as the same proteins in cancer tissues in Cy5 images. The volume of each spot was calculated using the BVA module of DeCyder software and represented graphically. The representative spot pairs of up-regulated (spots no. 1237, 1752, and 1839) and down-regulated (spot no. 1563) proteins in CCA tissue in comparison with MC are shown. The upper panel shows the images of the spots in the 2-D gels, and the lower panel shows the 3-D view of the corresponding spots. The calculated spot volumes are indicated under each image.

Table 2. Differentially expressed proteins in human ovarian cancer tissues

Spot no.	Protein name	Volume ratio (CCA/MA)
Up-regulation (more than 1.5-fold)		
1184	Tryptophanyl-tRNA synthetase	2.7
1237	Glutamate carboxypeptidase-like protein 1	3.1
1574	Macrophage capping protein	1.5
1752	L-lactate dehydrogenase B chain	2.2
1839	Annexin A4	7.6
1849	Purine nucleoside phosphorylase	2.7
1944	Prohibitin	2.3
1997	Ran-specific GTPase-activating protein	1.6
Down-regulation (more than 1.5-fold)		
1181	D-3-phosphoglycerate dehydrogenase	−2.9
1563	(Not identified)	−1.6
1804	Annexin A3	−4.8

shown in Table 2. Additionally, the representative spot images (three up-regulated and one down-regulated spot) in a 2-D gel and 3D-view simulations by DeCyder software are shown in Fig. 7.

4 Discussion

Epithelial ovarian cancer is one of the crucial diseases in women. Among the various types of epithelial ovarian cancer, CCA is one of the most malignant phenotypes with a high mortality rate, because of its chemoresistance and highly invasive character. If there were reliable biomarkers for detection of malignant ovarian cancer, such as CCA, in earlier stages, more appropriate clinical treatment could be administered and the mortality rate would be improved. However, the currently accepted serum marker, CA-125 lacks the sensitivity in some types of ovarian cancer, including CCA. Although some reports have described new biomarkers that may take the place of CA-125 [30], there have been no reports that focused on proteins characteristically expressed in malignant ovarian cancer types that might be used as diagnostics markers and/or target molecules for therapy. With the aim of improving the success rate of treatment, we have used proteomic analysis in this study to discover characteristically expressed proteins in ovarian cancer CCA. Recently developed 2-D DIGE techniques that use labeled proteins with three fluorescent dyes make it possible to detect expression differences, including proteins expressed in low amounts, with good accuracy [24]. Considering these advantages, our study was based on this technique.

In order to find new biomarkers, the samples for analysis can be prepared directly from tissue samples, but this strategy may contaminate the samples with proteins derived from blood fluids. To avoid this problem, we performed the differential analysis on cultured ovarian cancer cells. Cultural artifacts such as bovine serum proteins were washed out entirely with PBS before extraction. Using this approach, we were able to isolate and identify the considerable protein spots on 2-D gels that differentially changed in volumes between the two types of ovarian cancer. In our study, OVISE and OVTOKO were used as models of the malignant ovarian cancer type CCA. Both the CCA cells established from surgically extirpated CCA tissue specimens retained the original pathogenic characteristics such as chemoresistance and

heterotransplantation. On the other hand, there were two principal biological differences between these cells: (i) The OVISE cells shed tumor-associated antigens CA19–9, CA-125, and tissue polypeptide antigen in the culture medium, whereas the OVTOKO cells did not secrete them at detected level. (ii) Intraperitoneal transplantation of the OVTOKO cells occur distant metastasis, whereas that of the OVISE cells showed no dissemination and metastasis [23]. Additionally, as a control for another type of epithelial cancer, MCAS, which was the widely used cell line, was used in our study. The mucinous cystadenocarcinoma of MCAS is one of the frequently identifying type in clinical cases.

By analyzing the protein volumes from the data of 2-D DIGE images, we observed comparative expression profiles of 870 proteins among the three ovarian cancer cell lines. The results, depicted in Fig. 3, indicate that many proteins show large differences in expressions, not only between CCA and MCAS but also between the two CCA cell lines. Further analysis on relatively abundant proteins showed that 5.4–7.4% (MCAS, 31; OVISE, 24; and OVTOKO, 32) of the spots were significantly increased or decreased (>two-fold) in each cell line in comparison with the other cell lines (Fig. 4). These spot-volume analysis data indicated that many protein expressions were changed individually in each cell line, and that some of those proteins might decide the character of the cells while others were the results of the character transformation. It may be expected that some of the proteins indicating characteristic expression changes in CCA include factors related to malignancy, which would include them among potential diagnostics and/or therapeutic targets.

Some of the proteins of interest were identified by MS/MS analysis and are listed in Table 1. It is noteworthy that some of these selected proteins have already been reported as changing in their expressions in ovarian and/or other cancers by examinations using clinical tissue or fluid specimens. It has also been reported previously that in surgical specimens prepared from ovarian invasive carcinomas by 2-D analysis the up- and down-regulated proteins in the two CCA cell lines changed in tandem with increases in elongation factor 2 (EF-2) and triosephosphate isomerase levels, as well as decreases in cytokeratin 8 and 18 levels [31]. Elevated levels of GST P have been found in serum and plasma from patients with gastrointestinal, lung or bladder cancer [32–35], and have been demonstrated as a potentially useful prognostic factor for nonHodgkin's lymphoma at advanced stages [36]. The overexpression of peroxiredoxin I, which is a thiol-containing protein with efficient antioxidant capacity, was observed in oral cancer and mesothelioma specimens by immunohistochemistry [37, 38]. In addition, we were able to see some other proteins that have been observed in alternative expressions in samples prepared from various cancers.

EF-2 is listed not only as an up-regulated but also as a down-regulated protein in Table 1. This apparent discrepancy occurred because four horizontally located spots were all identified as EF-2. Among the four spots, one acidic form (Spot no. 582) was found to be increased and one basic form (Spot no. 584) was decreased in both CCA cell lines, compared with the mucinous adenocarcinoma cell line, MCAS. EF-2 catalyzes the last step of the elongation cycle in protein biosynthesis, and there are two PTMs, ADP-ribosylation and phosphorylation [39, 40]. These modifications cause the p*I* to drift. Additionally, these protein modifications reduce the affinity for the pretranslocation type of ribosome and are thus unable to promote translocation, which leads to the reduced function of EF-2 in protein synthesis [41, 42]. The multiple spots observed on our 2-D gels were considered to be due to the PTMs of this molecule because of the differences in p*I* [43], and the alternative pattern may indicate differences in the states of protein synthesis between the two cancer cell types.

Annexin A4 was also identified in two forms, one was overexpressed in both CCA cell lines, and the other was increased 22-fold only in the OVISE cell line in comparison with MCAS. Recently, this molecule has been found as an overexpressed protein in invasive renal cell carcinoma tissue [44, 45], pancreatic ductal adenocarcinoma tissue [46], and other cancer tissues. Annexin A4 belongs to an annexin family that contains calcium-dependent phospholipid binding proteins, and it can exist as a soluble protein as well as a membrane-associated protein [47]. Its function may be associated with membrane-related events along exocytotic and endocytotic pathways. Additionally, it seems possible that annexin A4 plays an important role in the morphological diversification and dissemination of the cancer cells through an alteration of its cell adhesion function, which is linked to one of the malignant characters of metastasis. But these are still not clearly defined, and may be contained in multiple spots observed in the 2-D analysis. Furthermore, a member of the annexin family, annexin A3, was found as a down-regulated protein in CCA cell lines. Consequently, this molecule deserves further study.

From these results, it is demonstrated that almost all of the spots identified as characteristic expression differences between the two types of cell lines by 2-D DIGE analysis have been in one way or another related to cancer diseases in previous studies. Because we expect that some of these molecules may have potential as markers of progression of malignancy of CCA, we preliminarily investigated their expression and differences in cancer tissues extirpated from patients with CCA. Mucinous cystadenoma tissue served as a disease control. The 2-D DIGE data obtained from this feasibility study indicated that some of the enclosed proteins were actually expressed in cancer tissues at the same migrated positions on 2-D gels as the corresponding proteins from the cultured cells. Additionally, some of these spots changed in the expression volumes in accordance with the results from culture cells.

Nevertheless, our validation study using cancer tissue was carried out with only limited samples, and the tissue samples have been contaminated with many other cells besides the aggressive malignant cells of CCA. Further

investigation, including the validation using many tissue samples, is necessary to find new useful biomarkers and/or therapeutic target molecules for malignant ovarian cancer, CCA. However, we have demonstrated that the present strategy, which includes the differential analysis using the cultural cell lines established from malignant CCA, can be used to generate the selected candidate proteins by 2-D DIGE. The analysis using tissue samples and the candidate validation of potential differentially regulated proteins is ongoing, and we aim to define the relationship between the functions of these proteins and progression of CCA.

5 References

[1] Bray, F., Loos, A. H., Tognazzo, S., La Vecchia, C., *Int. J. Cancer* 2005, *113*, 977–990.

[2] Tamakoshi, K., Kondo, T., Yatsuya, H., Hori, Y. *et al.*, *Gynecol. Oncol.* 2001, *83*, 64–71.

[3] Ioka, A., Tsukuma, H., Ajiki, W., Oshima, A., *Cancer Sci.* 2003, *94*, 292–296.

[4] Sugiyama, T., Kamura, T., Kigawa, J., Terakawa, N. *et al.*, *Cancer* 2000, *88*, 2584–2589.

[5] Sjövall, K., Nilsson, B., Einhorn, N., Jobo, T. *et al.*, *Gynecol. Oncol.* 2002, *85*, 175–178.

[6] Jobo, T., Sato, R., Kuramoto, H., *Rinsho Byori* 2003, *51*, 1188–1194.

[7] Bast, R. C., Jr., Klug, T. L., St John, E., Jenison, E. *et al.*, *New Engl. J. Med.* 1983, *309*, 883–887.

[8] Bast, R. C., Jr., Siegal, F. P., Runowicz, C. *et al.*, *Gynecol. Oncol.* 1985, *22*, 115–120.

[9] Bast, R. C., Jr., Knapp, R. C., *Eur. J. Obstet. Gynecol. Reprod. Biol.* 1985, *19*, 354–356.

[10] Meyer, T., Rustin, G. J., *Br. J. Cancer* 2000, *82*, 1535–1538.

[11] Merchant, M., Weinberger, S. R., *Electrophoresis* 2000, *21*, 1164–1177.

[12] Weinberger, S. R., Dalmasso, E. A., Fung, E. T., *Curr. Opin. Chem. Biol.* 2002, *6*, 86–91.

[13] Issaq, H. J., Veenstra, T. D., Conrads, T. P., Felschow, D., *Biochem. Biophys. Res. Commun.* 2002, *292*, 587–592.

[14] Ardekani, A. M., Liotta, L. A., Petricoin, E. F., *Expert Rev. Mol. Diagn.* 2002, *2*, 312–320.

[15] Vlahou, A., Schorge, J. O., Gregory, B. W., Coleman, R. L., *J. Biomed. Biotechnol.* 2003, *2003*, 308–314.

[16] Liotta, L. A., Petricoin, E. F., Ardekani, A. M. *et al.*, *Gynecol. Oncol.* 2003, *88*, S25–S28.

[17] Rai, A. J., Zhang, Z., Rosenzweig, J., Shih, I. *et al.*, *Arch. Pathol. Lab. Med.* 2002, *126*, 1518–1526.

[18] Zhang, Z., Bast, R. C., Jr., Yu, Y., Li, J. *et al.*, *Cancer Res.* 2004, *64*, 5882–5890.

[19] Alexe, G., Alexe, S., Liotta, L. A., Petricoin, E. F. *et al.*, *Proteomics* 2004, *4*, 766–783.

[20] Petricoin, E. F., Ardekani, A. M., Hitt, B. A., Levine, P. J. *et al.*, *Lancet* 2002, *359*, 572–577.

[21] Jones, M. B., Krutzsch, H., Shu, H., Zhao, Y. *et al.*, *Proteomics* 2002, *2*, 76–84.

[22] Ahmed, N., Barker, G., Oliva, K. T., Hoffmann, P. *et al.*, *Br. J. Cancer* 2004, *91*, 129–140.

[23] Gorai, I., Nakazawa, T., Miyagi, E., Hirahara, F. *et al.*, *Gynecol. Oncol.* 1995, *57*, 33–46.

[24] Yan, J. X., Devenish, A. T., Wait, R., Stone, T. *et al.*, *Proteomics* 2002, *2*, 1682–1698.

[25] Nakazawa, T., Gorai, I., Doi, C., Hirahara, F. *et al.*, *J. Jpn. Soc. Clin. Cytol.* 1992, *31*, 966–972.

[26] Alban, A., David, S. O., Bjorkesten, L., Andersson, C. *et al.*, *Proteomics* 2003, *3*, 36–44.

[27] Laemmli, U. K., *Nature* 1970, *227*, 680–685.

[28] Iwafune, Y., Kawasaki, H., Hirano, H., *Electrophoresis* 2002, *23*, 329–338.

[29] Miki, H. H., Yamanaka, Y., Nakamura, S., Kurata, S. *et al.*, *Sex Plant Rep.* 2004, *16*, 209–214.

[30] Jacobs, I. J., Menon, U., *Mol. Cell. Proteomics* 2004, *3*, 355–366.

[31] Alaiya, A. A., Franzen, B., Fujioka, K., Moberger, B. *et al.*, *Int. J. Cancer* 1997, *73*, 678–683.

[32] Niitsu, Y., Takahashi, Y., Saito, T., Hirata, Y. *et al.*, *Cancer* 1989, *63*, 317–323.

[33] Howie, A. F., Douglas, J. G., Fergusson, R. J., Beckett, G. J. *et al.*, *Clin. Chem.* 1990, *36*, 453–456.

[34] Tsuchida, S., Sekine, Y., Shineha, R., Nishihira, T. *et al.*, *Cancer Res.* 1989, *49*, 5225–5229.

[35] Berendsen, C. L., Mulder, T. P., Peters, W. H., *J. Urol.* 2000, *164*, 2126–2128.

[36] Katahira, T., Takayama, T., Miyanishi, K., Hayashi, T. *et al.*, *Clin. Cancer Res.* 2004, *10*, 7934–7940.

[37] Yanagawa, T., Iwasa, S., Ishii, T., Tabuchi, K. *et al.*, *Cancer Lett.* 2000, *156*, 27–35.

[38] Kinnula, V. L., Lehtonen, S., Sormunen, R., Kaarteenaho, W. R. *et al.*, *J. Pathol.* 2002, *196*, 316–323.

[39] Lavergne, J. P., Marzouki, A., Reboud, A. M., Reboud, J. P. *et al.*, *Biochim. Biophys. Acta* 1990, *1048*, 231–237.

[40] Ovchinnikov, L. P., Motuz, L. P., Natapov, P. G., Averbuch, L. J. *et al.*, *FEBS Lett.* 1990, *275*, 209–212.

[41] Nygard, O., Nilsson, L., *Biochim. Biophys. Acta* 1985, *824*, 152–162.

[42] Riis, B., Nygard, O., *FEBS Lett.* 1997, *407*, 21–24.

[43] Jäger, D., Seliger, C., Redpath, N. T., Friedrich, I. *et al.*, *Electrophoresis* 2000, *21*, 2729–2736.

[44] Shi, T., Dong, F., Liou, L. S., Duan, Z. H. *et al.*, *Mol. Carcinog.* 2004, *40*, 47–61.

[45] Zimmermann, U., Balabanov, S., Giebel, J., Teller, S. *et al.*, *Cancer Lett.* 2004, *209*, 111–8.

[46] Sitek, B., Luttges, J., Marcus, K., Kloppel, G. *et al.*, *Proteomics* 2005, *5*, 2665–2679.

[47] Gerke, V., Creutz, C. E., Moss, S. E., *Nat. Rev. Mol. Cell. Biol.* 2005, *6*, 449–461.

Mol Gen Genomics (2006) 275: 97–104
DOI 10.1007/s00438-005-0067-7

ORIGINAL PAPER

Hidenori Sassa · Hisashi Hirano

Identification of a new class of pistil-specific proteins of *Petunia inflata* that is structurally similar to, but functionally distinct from, the self-incompatibility factor HT

Received: 30 March 2005 / Accepted: 24 October 2005 / Published online: 1 December 2005

Abstract Pollen–pistil interactions are thought to involve a wide variety of intercellular recognition events controlled by diverse proteins and other molecules. One of the best characterized interactions is the S-RNase-based gametophytic self-incompatibility (GSI) system found in Solanaceae, Rosaceae and Scrophulariaceae. Although the *S* specificity of the pistil and the pollen in these families is determined by the *S* locus-encoded proteins S-RNase and SLF/SFB, respectively, these proteins alone are not sufficient for operation of the GSI reaction. Other factors are also required and are classified into three groups. To date, the only known factor is the pistil-expressed small asparagine-rich protein HT-B in three solanaceous genera *Nicotiana*, *Lycopersicon* and *Solanum*. HT-B is a Group 2 factor that is required for pollen rejection but do not affect S-RNase expression; factors in the other groups have not yet cloned. Here, we identified a new class of HT-like proteins in the style of *Petunia inflata* and named it HTL. Through alternative splicing, it was found that two isolated homologous *HTL* cDNAs, *HTL-A* and *HTL-B*, derived from a single gene. Like HT-B, HTL showed pistil-specific accumulation as well as significant sequence similarity to HT including conserved cystein residues at the C-terminal region and a signal peptide for extracellular localization. However, unlike HT-B, HTL lacked an asparagine-rich domain. Thus, it represents a new class of HT proteins. To determine whether HTL is involved in GSI function, RNA silencing constructs for HTL-A and HTL-B were introduced into self-incompatible *P. inflata*. Although several transgenic lines showed no detectable levels of both *HTL-A* and *HTL-B* transcripts, they retained normal GSI function and produced large fruits upon compatible pollination. This suggests that since silencing of the *HTL* gene alone is not sufficient to affect reproductive physiology, the gene is functionally distinct from the GSI factor *HT-B*.

Keywords *Petunia* · Pollen–pistil interactions · RNA silencing · Self-incompatibility

Communicated by G. Jürgens

Present address: H. Sassa (✉)
Faculty of Horticulture, Chiba University, Matsudo 648, 271-8510 Matsudo, Japan
E-mail: sassa@faculty.chiba-u.jp
Tel.: +81-47-3088967
Fax: +81-47-3088720

H. Hirano · H. Sassa
Kihara Institute for Biological Research, Yokohama City University, Maioka 641-12, Totsuka-ku, 244-0813 Yokohama, Japan

Introduction

Pollen–pistil interactions represent a critical step in the successful reproduction of plants. Through the interactions, the pistil rejects undesirable pollen while allows desirable, compatible pollen to grow for fertilization. While it is thought that various molecules in both the pistil and the pollen are involved in these cell–cell recognition mechanisms, little is known about their identities and roles.

The most characterized pollen–pistil interaction is self-incompatibility (SI), which promotes out-crossing by enabling the pistil to reject genetically related pollen. The dominant class of SI is gametophytic SI (GSI) which is, in general, controlled by a multiallelic locus *S*; when the *S* allele of the pollen matches one of the two *S* alleles of the pistil, then the pollen is recognized to be self and is rejected (de Nettancourt 2001; McCubbin and Kao 2000). The molecular basis of the *S* specificity of GSI has been extensively studied in Solanaceae, Rosaceae and Scrophulariaceae. *S* specificity in both the pistil and the pollen is controlled by distinct but tightly linked genes at the *S* locus, pistil-*S* and pollen-*S*, respectively. The pistil-*S* product is a ribonuclease called S-RNase, which is thought to act as a cytotoxin to the self pollen tube (McClure et al. 1989, 1990; Anderson et al. 1986; Lee et al. 1994; Murfett et al. 1994; Xue et al. 1996; Sassa et al. 1992, 1996, 1997; Broothaerts et al. 1995).

The product of pollen-*S* was unclear until very recently when molecular characterization of the *S* locus regions identified two F-box proteins, SFB and SLF, as pollen-*S* candidates (Lai et al. 2002; Entani et al. 2003; Qiao et al. 2004; Ushijima et al. 2003; Yamane et al. 2003). Further functional analysis showed that the *Petunia* F-box protein PiSLF encodes the *S* specificity of the pollen (Sijacic et al. 2004). Furthermore, Ushijima et al. (2004) and Sonneveld et al. (2005) showed that mutant *S* haplotypes of *Prunus* that confer pollen-specific self-compatibility are defective in the *SFB* gene, strongly supporting that *SFB* is the long sought after pollen-*S* gene.

Although the *S* specificity is exclusively controlled by the *S* locus products, genetic analyses also have shown that the *S* locus alone is not sufficient to operate GSI function; other factors are also required (Ai et al. 1991; Bernatzky et al. 1995; Hosaka and Hannemen 1998a, b). McClure et al. (2000) has classified these factors into three groups according to their functions. Group 1 factors directly affect the expression of *S*-specificity genes. Group 2 factors interact, either genetically or biochemically, with the specificity determinants and are required for pollen rejection but have no wider role in pollination. Group 3 factors include genes that function both in pollen rejection and in other pollen–pistil interactions (McClure et al. 2000). To date, the only factor characterized at the molecular level is the pistil-expressed small protein HT found in three solanaceous genera *Nicotiana*, *Lycopersicon* and *Solanum* (McClure et al. 1999; Kondo et al. 2002a, b; O'Brien et al. 2002). HT, which is characterized by an asparagine-rich region at the C-terminal and shows no significant homology to other proteins and, thus represents a new protein family (McClure et al. 1999). Although its biochemical function is not clear, HT is necessary for the pistil to reject self pollen (McClure et al. 1999; O'Brien et al. 2002). In *Solanum* and *Lycopersicon*, two highly related proteins, HT-A and HT-B, are found in a single species (Kondo et al. 2002a, b; O'Brien et al. 2002). In comparison to HT-B's amino acid sequence, HT-A has a small deletion at the terminus of the mature protein. RNA silencing experiments showed that the pistil requires expression of HT-B but not HT-A for GSI function (O'Brien et al. 2002). To date, only HT-B has been found in *Nicotiana*. The biological role of HT-A is not yet known. In other solanaceous genera with S-RNase information such as *Petunia* and *Physalis*, involvement of HT in GSI is not yet clarified. Since HT does not affect the expression of S-RNase, it is an example of a Group 2 factor (McClure et al. 2000). Although some S-RNase binding proteins are possible candidates for Group 3 factors in *Nicotiana* (McClure et al. 2000; Cruz-Garcia et al. 2005), molecular information about these proteins and their role in pollen rejection is still limited.

Characterization of the proteins/genes expressed in pistils and pollen are important for understanding the molecular networking of GSI and other pollen rejection mechanisms. Here, we describe identification of two new HT-like proteins from the pistils of self-incompatible *Petunia inflata*, HTL-A and HTL-B (for HT-like protein A and B, respectively). HTLs show a sequence homology to HT but lack the asparagine-rich region; thus, they represent a new class of HT proteins. RNA silencing experiments showed that loss of *HTL* expression is not sufficient for affecting either self-incompatible or compatible reactions.

Materials and methods

Plant material

Petunia inflata seeds were obtained from Dr. J.B. Power (University of Nottingham, UK). RT-PCR and RACE (Rapid Amplification of cDNA Ends; Frohman et al. 1988) procedures were used to isolate the two S-RNase encoding cDNAs S^{3L} and S^{k1} (DDBJ accession numbers AB094599 and AB094600, respectively). The S^{3L}-RNase sequence was identical to the reported S^3-RNase cDNA of *P. inflata* (Ai et al. 1990) with the exception of a single nucleotide difference that leads to the amino acid change of 135th valine residue (GTG) to leucine (CTG). A young flower bud of a petunia plant was pollinated to produce a selfed population, which was used to test the inheritance of the S^{3L}- and S^{k1}-RNase genes. Genomic fragments of the RNase genes (ca. 400 b) were amplified by REDExtract-N-Amp Plant PCR kit (SIGMA, St. Louis, MO, USA) with a primer pair of FSSR1 (5′-ATGATCTGGAACGCCACTGG-3′) and RSSR1 (5′-CTTCGTGCTGTCCGTTTCATC-3′), and then treated with *Eco*T22I to cut S^{k1} but not S^{3L}. Segregation of the RNase genotypes fitted the expected 1:2:1 ratio, indicating that they are allelic ($S^{3L}S^{3L}$:$S^{3L}S^{k1}$:$S^{k1}S^{k1}$ = 7:25:16, $0.100 < P < 0.250$). A mature flower of the $S^{3L}S^{3L}$ homozygous plant was pollinated by an $S^{3L}S^{k1}$ heterozygous plant, and the RNase genotypes of the 21 progenies determined. The genotypes were all $S^{3L}S^{k1}$. Since the S^{3L} pollen was rejected by the $S^{3L}S^{k1}$ pistil, this confirms that the cloned genes are alleles of the *S* locus. Progenies of $S^{k1}S^{k1} \times S^{3L}S^{k1}$ were all $S^{3L}S^{k1}$ (16 plants), providing further support that the clones correspond to S-RNases.

Cloning of cDNA and genomic fragment

Total RNA was extracted from the pistils of *P. inflata* ($S^{3L}S^{3L}$), and reverse transcribed with a $d(T)_{17}$ adapter primer to generate cDNA as described in Sassa and Hirano (1998) and Ushijima et al. (2003). A PCR primer (FHT1, 5′-GTTCTTTTGATAATATCATCAG-3′) was designed on the basis of an alignment of reported *HT* sequences. The primer was designed to amplify the *HT*-like sequence of petunia by a 3′RACE with *ExTaq* DNA polymerase (Takara, Otsu, Japan) using the cDNA template and the 24-mer adapter sequence at the 3′ (Sassa and Hirano 1998). Primers RHT2 (5′-ACTTTTACTG CAGTACCCATG-3′) and R2PiHT1 (5′-TTACAA

CAGTTACATTCTTGGC-3′) were used for 5′RACE of HTL-A and HTL-B, respectively. A 3′RACE for amplification of full-length cDNAs for HTL-A and HTL-B was conducted using both an FPHT (5′-AGA ATTTATTCATCAAAATGG-3′) as a gene-specific primer, and a high fidelity DNA polymerase *Pyrobest* (Takara). The PCR products were cloned into a pZErO-2 vector (Invitrogen, Carlsbad, CA, USA) and sequenced. The deduced amino acid sequences of petunia proteins were aligned with those of solanaceous HT proteins by using ClustalX with default parameter settings (Thompson et al. 1997). Phylogenetic tree of HT-like proteins was generated from the alignment by neighbor-joining method (Saitou and Nei 1987). Bootstrap analysis was performed for 1,000 replicates.

Genomic fragments of *HTL-A* and *HTL-B* genes were amplified from *P. inflata* DNA by a *Pyrobest* DNA polymerase with the primer pairs FPHT and RPHTPT15 (5′- CGCGGATCCTTAGGAAGAACA TTTTTTAATAC-3′), and FPHT and R2PiHT1, respectively. They were then cloned and sequenced.

Gel blot analysis of DNA and RNA

Genomic DNA of *P. inflata* was extracted as described in Doyle and Doyle (1990). Ten microgram of DNA were digested by restriction enzymes, separated in an agarose gel, blotted onto a nylon membrane (Biodyne Plus; Pall), and hybridized with digoxygenin (DIG) labeled probes as described in Sassa and Hirano (1998).

Pistil RNA from both wild type and transgenic lines was extracted. Ten microgram were separated in a formaldehyde gel, blotted onto a nylon membrane and hybridized with DIG-labeled probes as described in Sassa et al. (1997). The probes specific to the *HTL-A* and *HTL-B* genes were amplified from their respective 3′RACE clones using FAHTmHlf (5′-CAAATGAT-CAACGCCAGAACAC-3′) and a vector-derived primer M13-47 (5′-CGCCAGGGTTTTCCCAGTCACGAC 3′) and FBHTmHlf (5′- CAAATGAAGGGCTGAA CACAAG-3′) and M13-47, respectively.

Expression in *E. coli*, production of antiserum and immunoblot analysis

The coding region of HTL-A was amplified from the cDNA clone using FPHTPT15 (5′-GAAAGTA TCATATGGTTGCTGCTAGGGAAATAAC-3′) and RPHTPT15 (5′-CGCGGATCCTTAGGAAGAACATT TTTTAATAC-3′) with a *Pyrobest* DNA polymerase. It was then digested by *Nde*I and *Bam*HI and cloned into pET15b (Novagen, Darmstadt, Germany) to generate pETPiHTLA. pETPiHTLA was transferred to an *E. coli* strain Rosetta-gami (DE3) (Novagen) to express a recombinant HTL-A protein. This recombinant HTL-A protein was recovered from an insoluble fraction by solubilization in 8 M urea and was purified by adsorption to a HiTrap Chelating column according to the manufacture's instruction (AmershamBioscience Corp., Piscataway, NJ, USA). The HTL-A protein was further separated into SDS-PAGE gels, recovered by electroelution and used to immunize a rabbit to obtain antiserum as described in Sassa and Hirano (1998).

Proteins were extracted from the various floral organs and leaves of *P. inflata* with an extraction buffer (8 M urea, 50 mM Tris–HCl pH 6.8, 0.2% 2-mercaptoethanol) and quantified by the method described in Bradford (1976). Equal volumes of 2x SDS-sample buffer (125 mM Tris–HCl pH 6.8, 5% SDS, 10% 2-mercaptoethanol, 20% glycerol) were mixed and loaded to Tricine SDS–PAGE gel as described in Schägger and von Jagow (1987). Separated proteins were transferred to a PVDF membrane and probed by the antiserum against recombinant HTLA protein as described in Sassa and Hirano (1998) and Ushijima et al. (2001).

RNA silencing

Self-complementary hairpin RNA-mediated gene silencing constructs were prepared by using pHANNIBAL (Wesley et al. 2001). The HTL-A coding region was amplified by a *Pyrobest* polymerase with FPHTHAN (5′-GCTCTAGACTCGAGTAGAATTTATTCATCA AAATGG-3′) and RPHTHAN2 (5′-GCATCGATGG TACCATCAGGTGTACAACATTGGC-3′) and was cloned into pHANNIBAL in sense and antisense orientation separated by *Pdk* intron (Wesley et al. 2001). The resultant silencing cassette was released by *Not*I digestion and moved to a binary vector pART27 (Gleave 1992) to create pARTHANHTLA. A silencing cassette for HTL-B was prepared by amplifying HTL-B cDNA with FPHTHAN and RHANPHTB (5′-GCATCGATGG TACCGAAGTTATTCAGGTCATTCC-3′) and by cloning it into pHANNIBAL as described. The HTL-B silencing cassette was excised by *Sac*I and *Spe*I, and inserted into *Sac*I–*Xba*I sites of pBINPLUS (van Engelen et al. 1995) to obtain pBINHANHTLB. The silencing constructs pARTHANHTLA and pBINHANHTLB were introduced to *Agrobacterium tumefaciens* LBA4404 to transform *P. inflata* ($S^{3L}S^{3L}$) by leaf disk method (Horsch et al. 1985).

Results

Isolation of a new class of *HT*-like genes from the pistils of *P. inflata*

Two homologous cDNA clones encoding HT-like proteins with 90 and 89 amino acid residues were obtained from the pistils of self-incompatible *P. inflata*. These clones were named *PiHTL-A* (acc # AB094602) and *PiHTL-B* (acc # AB158317) for *P. inflata* HT-like proteins. The SignalP analysis (Nielsen et al. 1997) predicted signal sequence cleavage before the 27th arginine

residue. The deduced amino acid sequences of HTL-A and HTL-B proteins showed 73% identity with each other and 19.3%–43.2% identity with the HT proteins of *Nicotiana*, *Lycopersicon* and *Solanum*. An amino acid sequence alignment is shown in Fig. 1a. Although PiHTLs showed sequence homologies to previously reported solanaceous HT proteins, they lacked the asparagine-rich region characteristic of the HT proteins. Thus, they represent a new class of HT proteins. Figure 1b shows that the closest protein to PiHTLs is *Nicotiana* HT. This may reflect a phylogenetic relationship of solanaceous species. *Petunia*, *Nicotiana*, *Lycopersicon* and *Solanum* belong to the subfamily Petunioideae, Nicotianoideae, Solanoideae and Solanoideae, respectively. Petunioideae is more closely related to Nicotianoideae than it is to Solanoideae (Olmstead et al. 1999).

Alternative splicing of the *HTL* gene

PCR amplification of *HTL* genes from genomic DNA gave larger products than those from pistil cDNA, suggesting the occurrence of intron(s) in the *HTL* genes (Fig. 2b). The genomic fragments of *HTL-A* and *HTL-B* were cloned and sequenced. Comparisons showed that the *HTL-A* genomic fragment contained an intron, and was incorporated in the *HTL-B* genomic sequence (acc # AB158318). These results indicate that *HTL-A* and *HTL-B* are alternative splicing products. Figure 2 a and c show the structure of the *HTL* gene. The joining of exon 1 and 2 produces the *HTL-A* transcript, and the joining of exon 1 and 3 gives rise to *HTL-B*. Genomic Southern blot analysis indicated that the *HTL* gene is a single copy in the petunia genome (Fig. 2d).

Organ-specific expression of the HTL protein

HTL-A cDNA was introduced to an expression vector pET15b. The resultant plasmid was transferred into *E. coli* to produce recombinant HTL-A protein, which was used to immunize a rabbit to obtain antiserum against the HTL protein. The antiserum, in turn, was used to determine whether HTL accumulated in specific organs

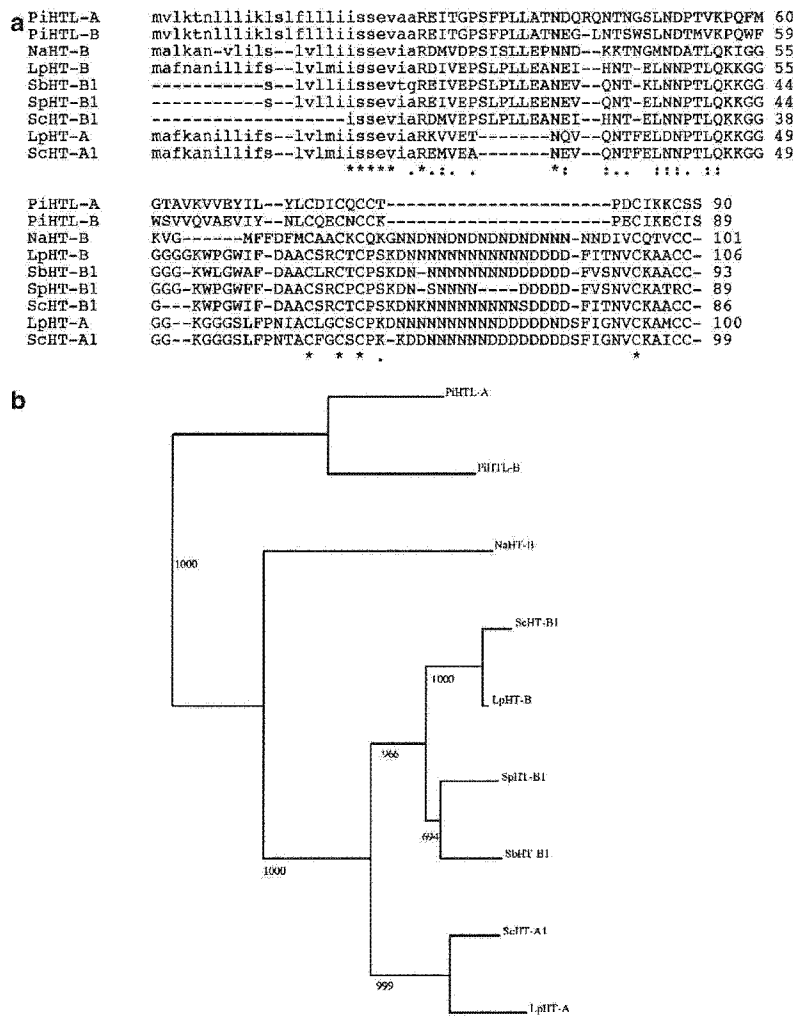

Fig. 1 Amino acid sequence alignment (**a**) and a phylogenetic tree (**b**) of HT and related proteins of the solanaceous species. a Protein sequences were aligned by ClustalX program (Thompson et al. 1997) for phylogenetic analysis with default parameter settings. Predicted signal peptides are shown in *lower case*. Amino acid identities of PiHTL-A with solanaceous HT proteins are 43.2% (NaHT-B), 36.9% (ScHT-B1), 41.2% (LpHT-B), 36.5% (SpHT-B1), 39.2% (SbHT-B1), 23.9% (ScHT-A1) and 19.3% (LpHT-A). **b** A neighbor-joining tree (Saitou and Nei 1987) of the HT and related proteins. *Numbers* denote bootstrap values with 1,000 replicates

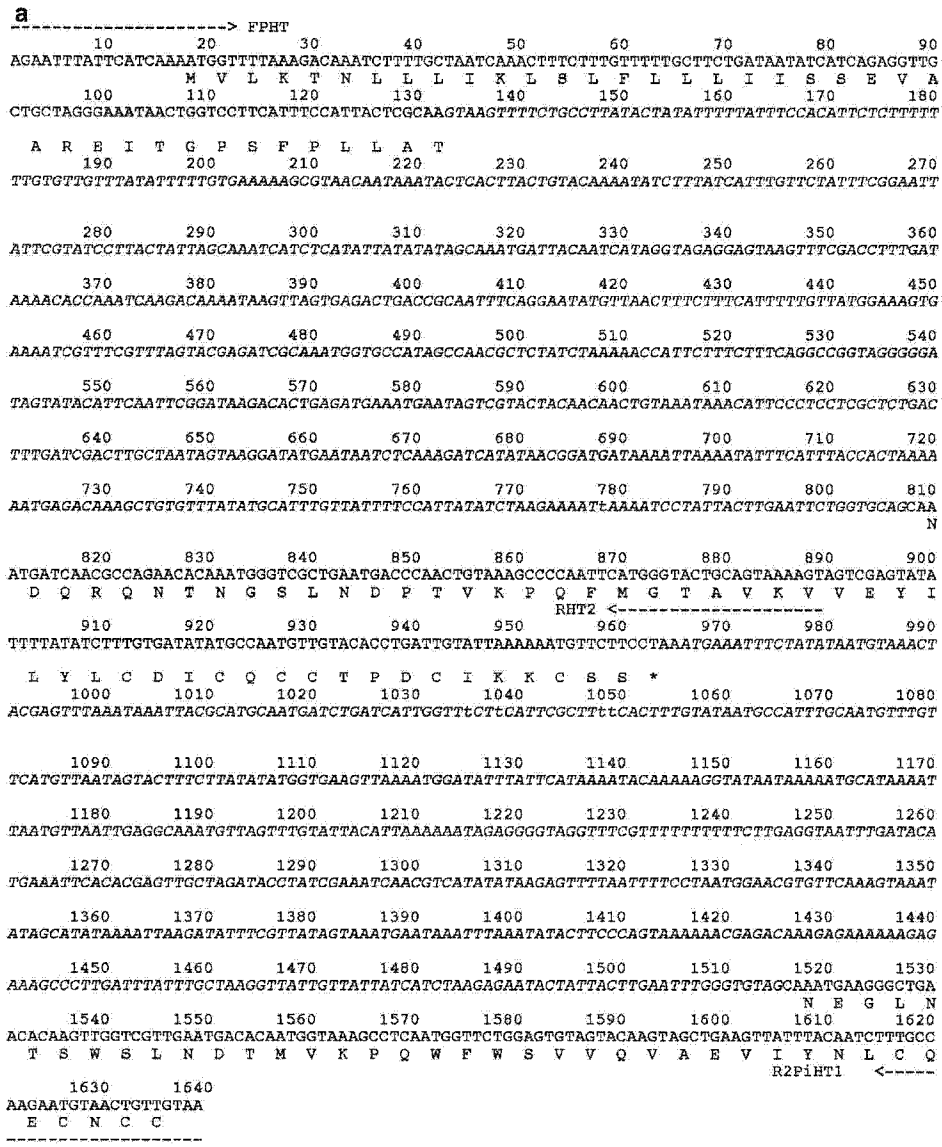

Fig. 2 Organization and alternative splicing of *PiHTL* gene. **a** Partial genomic sequence of *PiHTL* gene. The deduced amino acid sequence is shown under the nucleotide sequence. Intron sequences are in *italics*. Positions of the primers used for PCR analyses are indicated by *arrows*. **b** PCR amplification of *PiHTL* fragments from the pistil cDNA (*lane c*) and the genomic DNA (*lane g*). **c** Schematic representation of the structure and alternative splicing of the *PiHTL* gene (not proportional). *Boxes* and *lines* represent exons and introns, respectively. The *arrowhead* denotes the putative cleavage site of the signal peptide. **d** Genomic Southern blotting with a *PiHTL-B* cDNA probe

of *P. inflata*. Figure 3 shows the expression pattern of HTL proteins in the different organs. HTL proteins were found to be specific to styles; they did not accumulate in other floral organs and leaves, as other solanaceous HT proteins do. The several minor bands found in the style extract may reflect either post-translational modifications and/or occurrence of related protein(s).

Effect of *HTL* gene silencing on self-incompatible and compatible pollinations

To assess whether HTL proteins have a role in pollen–pistil interactions, RNA silencing constructs of HTL-A and HTL-B were introduced into self-incompatible *P. inflata* plants ($S^{3L}S^{3L}$ genotype) by the *Agrobacterium*-mediated method. Regenerated plants were analyzed by genomic Southern blot analysis with the *NPT* gene as a probe to confirm the integration of the T-DNA in the genome (data not shown). Nine plants transformed by the HTL-A-silencing construct and 11 plants transformed by the HTL-B-silencing construct were subjected to immunoblot analysis with the HTL-A antiserum. The transgenic plants showed different degrees of suppression of the HTL protein level, and were incompatible with self pollen (data not shown). None showed any morphological change (data not shown). Four transgenic plants with the HTL-A silencing construct (# 1, 3, 6 and 10) and four plants targeted for HTL-B (# 1, 8, 13 and 17) showed an extreme reduction in levels of HTL. The mRNA levels and pollination behaviors of these plants were analyzed. Style RNA was isolated from the selected transformants, and probed for *HTL-A* or *HTL-B*. The RNA gel blot analysis showed that all four

Fig. 2 (Contd.)

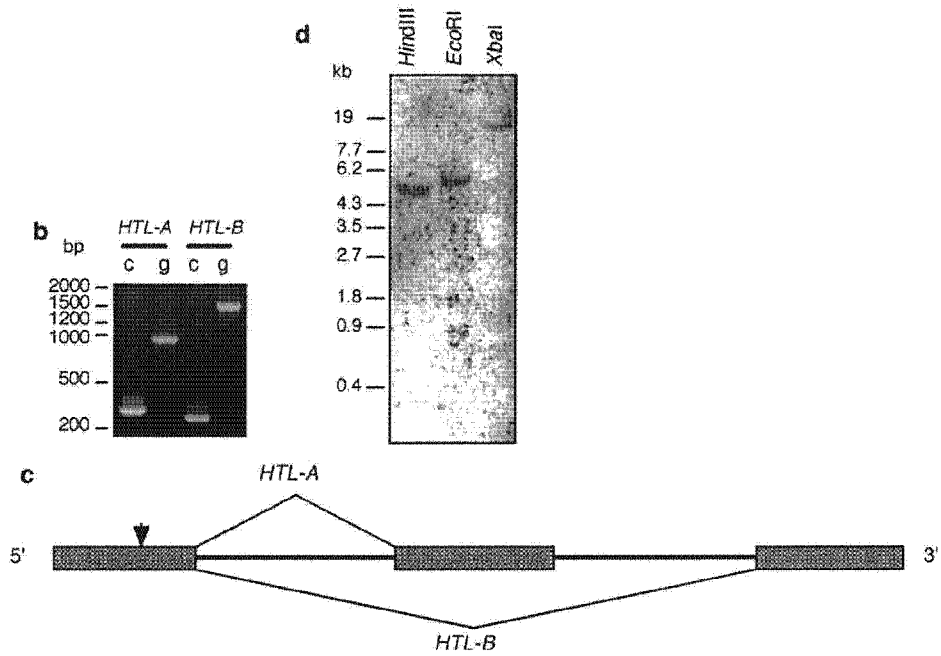

HTL-A silencing plants accumulated no detectable levels of both *HTL-A* and *HTL-B* transcripts. The HTL-B-targeted plants showed different levels of reduction of *HTL* transcripts (Fig. 4). The HTL-silencing plants with no detectable levels of *HTL* transcripts were either self-pollinated at the mature (self pollination; SP) or immature (bud pollination; BP) stage of floral bud development, or were pollinated with cross-compatible pollen (compatible pollination; CP) from $S^{k1}S^{k1}$ plants. All the transgenic lines and the untransformed plant bore big, small and no capsules upon cross-, bud- and self-pollination, respectively. This indicates that the transgenic plants are fertile both for male and female organs, and retain complete self-incompatibility function (Fig. 4).

Discussion

HTL-A and HTL-B are similar to the solanaceous HT proteins in terms of overall amino acid sequence, location of cystein residues, occurrence of putative signal

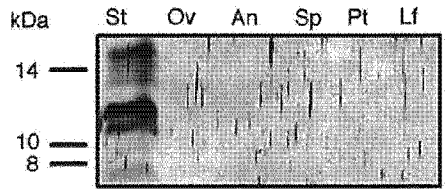

Fig. 3 Immunoblot analysis of the HTL protein in different organs of *P. inflata*. Fifteen micrograms of crude proteins from different organs were separated by Tricine SDS–PAGE, electroblotted onto a PVDF membrane, and probed by antiserum against PiHTL-A. *St* style, *Ov* ovary, *An* anther, *Sp* sepal, *Pt* petal, *Lf* leaf

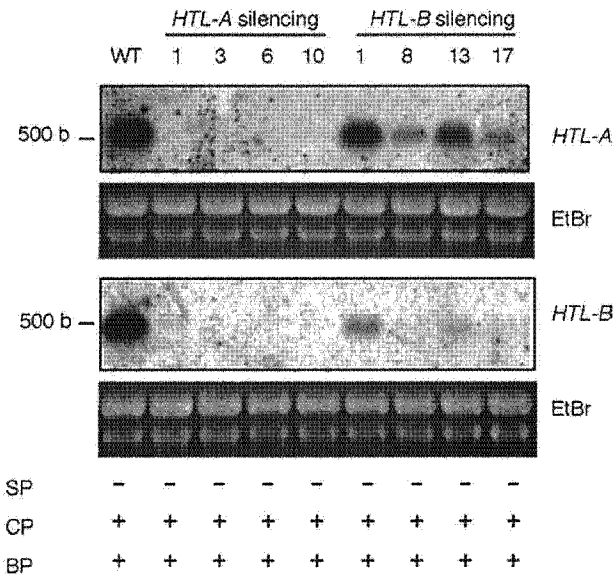

Fig. 4 RNA silencing of the *PiHTL* gene and its effect on incompatible and compatible pollination. Northern blot analysis of the *PiHTL* gene of RNA silencing transgenic plants. Plant number is denoted on each lane. Wild type (*WT*) plant is the untransformed host plant with the genotype of $S^{3L}S^{3L}$. Ten micrograms of total RNA from styles were loaded in each lane. The RNA blots were probed by 3′ half fragments of each *PiHTL* cDNA clone. Ethidiumbromide-stained gels were used to ensure equal loading. Fruit development of *PiHTL* silencing plants after incompatible and compatible pollinations were presented by *plus* (+, developed fruit) or *minus* (−, aborted ovary) signes. Mature and emasculated flower buds were pollinated by the neighbor flowers of the same plants (self-pollination *SP*) or by pollen from an $S^{k1}S^{k1}$ plant (cross-pollination *CP*). Young flower buds were emasculated and self-pollinated at ca. 3 days before anthesis (bud pollination *BP*). Pollinated flower buds were bagged to prevent further pollination and grown for 2 weeks, and assessed for fruit development

peptide and style-specific accumulation. In addition, it is noteworthy that the deletion of five to seven residues in the amino terminal region represents a structural characteristic for isoform A of HT (O'Brien et al. 2002), and that the corresponding region of petunia HTL is much closer to the GSI factor isoform B than the non-SI factor isoform A. However, the significant structural difference between the petunia HTLs and other HTs is the lack of the asparagine-rich region in HTL. Although the asparagine-rich region is retained in HT-A proteins which are known not to be involved in SI (O'Brien et al. 2002), its biological role is still unknown and may constitute a necessary part of the HT-B function in the operation of SI.

Genomic sequence analysis showed that two isoforms of petunia HTL are derived from alternative splicing of a single gene. Although *Solanum* and *Lycopersicon* express two isoforms of *HT* transcripts, the nucleotide differences between the isoforms of a single species are dispersed in the sequences (Kondo et al. 2002a, b; O'Brien et al. 2002). This and RFLP analysis of the genes by O'Brien et al. (2002) suggest that the isoforms are encoded by different genes. Generations of variants through alternative splicing may be a characteristic of *HTL*.

In order to determine whether HTL is involved in GSI function, RNA silencing plants for the *HTL* gene were produced. The hairpin RNA induced gene silencing strategy (Wesley et al. 2001) was found to be very effective in knocking down the expression of *HTL* gene. While some transgenic lines showed no detectable levels of accumulation of both *HTL-A* and *HTL-B* transcripts, the silenced plants showed no morphological change and retained normal self-incompatibility and compatibility behavior. One possibility is that HTL is redundantly involved in GSI with unidentified related protein(s) and that knock-down of HTL alone is not sufficient to change reproductive physiology. Identification and silencing of other *HT*-like gene(s) in petunia, comparison of it with the *HTL* silencing phenotype and, if necessary, production of simultaneous silencing plants for both *HT*-like genes will be needed to test this possibility.

It is also likely that HTL is required under specific conditions not tested in this study. One possibility may be the involvement of HTL in an incompatibile reaction against pollen from different species. Another possibility is that HTL is involved in the defense mechanism of the pistil against invasion of pathogens. While pistils are very rich in the nutrients required for pollen tube growth and are, thus, vulnerable to pathogen invasion, infection of the pistil is rare (Atkinson et al. 1993). This is consistent with the findings that pistils accumulate varieties of potential antimicrobial proteins such as defferent pathogenesis-related (PR) proteins (eg., Sassa and Hirano 1998). Sessa and Fluhr (1995) showed that the suppression of the pistil-specific glucanase (PR3) by antisense approach had no influence on reproductive physiology of tobacco, and postulated that the glucanase is involved in defense of the pistil. It is noteworthy that a tobacco S-like RNase (RNaseNE) inhibits hyphal elongation of plant pathogens; this represents an additional cytotoxic activity of the extracellular class of plant RNase beyond the cytotoxic effect of the S-RNase on self pollen in the GSI system (Hugot et al. 2002). Moreover, it is also interesting that the S-RNase-based cytotoxic effect against self-pollen requires HT-B and that the petunia pistil accumulates HTL and the S-like RNases, the latter being implicated in the defense mechanism of the pistil (Singh et al. 1991; Lee et al. 1992). Although HT-B is postulated to interact with pollen tubes and to facilitate uptake of S-RNase, its biochemical function in SI mechanism is not yet known (McClure et al. 1999). The elucidation of the precise role of any member of HT-like protein family will provide insight into the biochemical function of other members and help us better understand the pollen–pistil interactions.

Acknowledgments We thank Dr. J.B. Power for *P. inflata* seeds, Dr. P.M. Waterhouse for pHANNIBAL, Dr. A.P. Gleave for pART27 and Dr. W.J. Stiekema for pBINPLUS. Drs. Y. Ogawa, Y. Hoshino and H. Washida are acknowledged for their technical advice. We also thank Melody Kroll for proof reading this manuscript. This work was supported in part by the Grants-in-Aid for Scientific Research (C, 13660011) and the Grants-in-Aid for Young Scientists (A, 16688001) from the Ministry of Education, Science, Sports and Culture of Japan to H.S.

References

Ai Y, Singh A, Coleman CE, Ioerger TR, Kheyr-Pour A, Kao T-H (1990) Self-incompatibility in *Petunia inflata*: isolation and characterization of cDNAs encoding three S-allele-associated proteins. Sex Plant Reprod 3:130–138

Ai Y, Kron E, Kao T-H (1991) S-alleles are retained and expressed in a self-compatible cultivar of *Petunia hybrida*. Mol Gen Genet 230:353–358

Anderson MA, Cornish EC, Mau S-L et al (1986) Cloning of cDNA for a style glycoprotein associated with expression of self-incompatibility in Nicotiana alata. Nature 321:38–44

Atkinson AH, Heath RL, Simpson RJ, Clarke AE, Anderson MA (1993) Proteinase inhibitors in *Nicotiana alata* stigmas are derived from a precursor protein which is processed into five homologous inhibitors. Plant Cell 5(2):203–213

Bernatzky R, Glaven RH, Rivers BA (1995) *S*-related protein can be recombined with self-compatibility in interspecific derivatives of *Lycopersicon* (tomato). Biochem Genet 33:215–225

Bradford M (1976) A rapid and sensitive method for quantitation of microgram quantities of protein utilizing the principle of protein-dye binding. Anal Biochem 72:248–254

Broothaerts W, Janssens GA, Proost P, Broekaert WF (1995) cDNA cloning and molecular analysis of two self-incompatibility alleles from apple. Plant Mol Biol 27:499–511

Cruz-Garcia F, Hancock N, Kim D, McClure B (2005) Stylar glycoproteins bind to S-RNase *in vitro*. Plant J 42:295–304

de Nettancourt D (2001) Incompatibility and incongruity in wild and cultivated plants. Springer, Berlin Heidelberg New York

Doyle JJ, Doyle JL (1990) Isolation of plant DNA from fresh tissue. Focus 12:13–15

Entani T, Iwano M, Shiba H, Che F-S, Isogai A, Takayama S (2003) Comparative analysis of the self-incompatibility (*S*-) locus region of *Prunus mume*: identification of a pollen expressed F-box gene with allelic diversity. Genes Cells 8:203–213

Frohman MA, Dush MK, Martin GR (1988) Rapid production of full-length cDNAs from rare transcripts: amplification using single gene-specific oligonucleotide primer. Proc Natl Acad Sci USA 85:8998–9002

Gleave AP (1992) A versatile binary vector system with a T-DNA organisational structure conductive to efficient integration of cloned DNA into the plant genome. Plant Mol Biol 20:1203–1207

Horsch RB, Fry JE, Hoffmann NL, Eichholtz D, Rogers SG, Fraley RT (1985) A simple and general method for transferring genes into plants. Science 227:1229–1231

Hosaka K, Hannemen RE (1998a) Genetics of self-compatibility in a self-incompatible wild diploid potato species *Solanum chacoense*. 1. Detection of an *S* locus inhibitor (*Sli*) gene. Euphytica 99:191–197

Hosaka K, Hannemen RE (1998b) Genetics of self-compatibility in a self-incompatible wild diploid potato species *Solanum chacoense*. 2. Localization of an *S* locus inhibitor (*Sli*) gene on the potato genome using DNA markers. Euphytica 103:265–271

Hugot K, Ponchet M, Marais A, Ricci P, Galiana E (2002) A tobacco S-like RNase inhibits hyphal elongation of plant pathogens. Mol Plant Microbe Interact 15:243–250

Kondo K, Yamamoto M, Itahashi R, Sato T, Egashira H, Hattori T, Kowyama Y (2002a) Insights into the evolution of self-incompatibility in *Lycopersicon* from a study of stylar factors. Plant J 30:143–154

Kondo K, Yamamoto M, Matton DP, Sato T, Hirai M, Norioka S, Hattori T, Kowyama Y (2002b) Cultivated tomato has defects in both *S-RNase* and *HT* genes required for stylar function of self-incompatibility. Plant J 29:627–636

Lai Z, Ma W, Han B, Liang L, Zhang Y, Hong G, Xue Y (2002) An F-box gene linked to the self-incompatibility (*S*) locus of *Antirrhinum* is expressed specifically in pollen and tapetum. Plant Mol Biol 50:29–42

Lee H-S, Singh A, Kao T-H (1992) RNase X2, a pistil-specific ribonuclease from *Petunia inflata*, shares sequence similarity with solanaceous S proteins. Plant Mol Biol 20:1131–1141

Lee H-S, Huang S, Kao T-H (1994) S proteins control rejection of incompatible pollen in *Petunia inflata*. Nature 367:560–563

McClure BA, Haring V, Ebert PR, Anderson MA, Simpson RJ, Sakiyama F, Clarke AE (1989) Style self-incompatibility products of *Nicotiana alata* are ribonucleases. Nature 342:955–957

McClure BA, Gray JE, Anderson MA, Clarke AE (1990) Self-incompatibility in *Nicotiana alata* involves degradation of pollen rRNA. Nature 347:757–760

McClure B, Mou B, Canevascini S, Bernatzky R (1999) A small asparagine -rich protein required for S-allele-specific pollen rejection in *Nicotiana*. Proc Natl Acad Sci USA 96:13548–13553

McClure BA, Cruz-Garcia F, Beecher BS, Sulaman W (2000) Factors affecting inter- and intra-specific pollen rejection in Nicotiana. Ann Bot 85:113–123

McCubbin AG, Kao T-H (2000) Molecular recognition and response in pollen and pistil interactions. Annu Rev Cell Dev Biol 16:333–364

Murfett J, Atherton TL, Mou B, Gasser CS, McClure BA (1994) S-RNase expressed in transgenic *Nicotiana* causes *S*-allele-specific pollen rejection. Nature 367:563–566

Nielsen H, Engelbrecht J, Brunak S, von Heijne G (1997) Identification of prokaryotic and eukaryotic signal peptides and prediction of their cleavage sites. Protein Eng 10:1–6

O'Brien M, Kapfer C, Major G, Laurin M, Bertrand C, Kondo K, Kowyama Y, Matton DP (2002) Molecular analysis of the stylar-expressed *Solanum chacoense* small asparagine-rich protein family related to the HT modifier of gametophytic self-incompatibility in *Nicotiana*. Plant J 32:985–996

Olmstead RG, Sweere JA, Spangler RE, Bohs L, Palmer JD (1999) Phylogenetic and provisional classification of the Solanaceae based on chloroplast DNA. In: Nee M, Symon DE, Lester PN, Jessop JP (eds) Solanaceae IV. Royal Botanic Gardens, Kew, pp 111–137

Qiao H, Wang H, Zhao L, Zhou J, Huang J, Zhang Y, Xue Y (2004) The F-box protein AhSLF-S2 physically interacts with S-RNases that may be inhibited by the ubiquitin/26S proteasome pathway of protein degradation during compatible pollination in *Antirrhinum*. Plant Cell 16:571–581

Saitou N, Nei M (1987) The neighbor-joining method: a new method for reconstructing phylogenetic trees. Mol Biol Evol 4:406–425

Sassa H, Hirano H (1998) Style-specific and developmentally regulated accumulation of a glycosylated thaumatin/PR 5-like protein in Japanese pear (*Pyrus serotina* Rehd.). Planta 205:514 521

Sassa H, Hirano H, Ikehashi H (1992) Self-incompatibility-related RNases in styles of Japanese pear (*Pyrus serotina* Rehd.). Plant Cell Physiol 33:811–814

Sassa H, Nishio T, Kowyama Y, Hirano H, Koba T, Ikehashi H (1996) Self-incompatibility (*S*) alleles of the Rosaceae encode members of a distinct class of the T_2/S-ribonuclease superfamily. Mol Gen Genet 250:547–557

Sassa H, Hirano H, Nishio T, Koba T (1997) Style-specific self-compatible mutation caused by deletion of the S-RNase gene in Japanese pear (*Pyrus serotina*). Plant J 12:223–227

Schägger H, von Jagow G (1987) Tricine-sodium dodecyl sulfate-polyacrylamide gel electrophoresis for the separation of proteins in the range from 1 to 100 kDa. Anal Biochem 166:368–379

Sessa G, Fluhr R (1995) The expression of an abundunt transmitting tract-specific endoglucanase (Sp41) is promoter-dependent and not essential for the reproductive physiology of tobacco. Plant Mol Biol 29:969–982

Sijacic P, Wang X, Skirpan AL, Wang Y, Dowd PE, McCubbin AG, Huang S, Kao T-H (2004) Identification of the pollen determinant of S-RNase-mediated self-incompatibility. Nature 429:302–305

Singh A, Ai Y, Kao T-H (1991) Characterization of ribonuclease activity of three S-allele-associated proteins of *Petunia inflata*. Plant Physiol 96:61–68

Sonneveld T, Tobutt KR, Vaughan SP, Robbins T (2005) Loss of pollen-*S* function in two self-compatible selections of *Prunus avium* is associated with deletion/mutation of an *S* haplotype-specific F-box gene. Plant Cell 17:37–51

Thompson JD, Gibson TJ, Plewniak F, Jeanmougin F, Higgins DG (1997) The clustal X windows interface: flexible strategies for multiple sequence alignment aided by quality analysis tools. Nucleic Acids Res 25:4876–4882

Ushijima K, Sassa H, Tamura M, Kusaba M, Tao R, Gradziel TM, Dandekar AM, Hirano H (2001) Characterization of the *S*-locus region of almond (*Prunus dulcis*): analysis of a somaclonal mutant and a cosmid contig for an *S* haplotype. Genetics 158:379–386

Ushijima K, Sassa H, Dandekar AM, Gradziel TM, Tao R, Hirano H (2003) Structural and transcriptional analysis of the self-incompatibility locus of almond: identification of a pollen-expressed F-box gene with haplotype-specific polymorphism. Plant Cell 15:771–781

Ushijima K, Yamane H, Watari A, Kakehi E, Ikeda K, Hauck NR, Iezzoni AF, Tao R (2004) The *S* haplotype-specific F-box protein gene, *SFB*, is defective in self-compatible haplotypes of *Prunus avium* and *P. mume*. Plant J 39:573–586

van Engelen FA, Molthoff JW, Conner AJ, Nap J-P, Pereira A, Stiekema WJ (1995) pBINPLUS: an improved plant transformation vector based on pBIN19. Transgenic Res 4:288–290

Wesley SV, Helliwell CA, Smith NA, Wang MB, Rouse DT, Liu Q, Gooding PS, Singh SP, Abbott D, Stoutjesdijk PA, Robinson SP, Gleave AP, Green AG, Waterhouse PM (2001) Construct design for efficient, effective and high-throughput gene silencing in plants. Plant J 27:581–590

Xue Y, Carpenter R, Dickinson H, Coen ES (1996) Origin of allelic diversity in Antirrhinum S locus RNases. Plant Cell 8:805–814

Yamane H, Ikeda K, Ushijima K, Sassa H, Tao R (2003) A pollen-expressed gene for a novel protein with an F-box motif that is very tightly linked to a gene for S-RNase in two species of cherry, *Prunus cerasus* and *P. avium*. Plant Cell Physiol 44:764–769

RESEARCH ARTICLE

A novel approach and protocol for discovering extremely low-abundance proteins in serum

Yoshinori Tanaka[1], Hideo Akiyama[1], Toshihiko Kuroda[1], Giman Jung[1], Kazuhiro Tanahashi[2], Hiroyuki Sugaya[2], Jun Utsumi[3], Hiroshi Kawasaki[4] and Hisashi Hirano[4]

[1] Toray Industries, Inc., New Frontiers Research Laboratories, Kamakura, Kanagawa, Japan
[2] Toray Industries, Inc., Specialty Materials Research Laboratories, Otsu, Shiga, Japan
[3] Toray Industries, Inc., Corporate Research Department, Tokyo, Japan
[4] Yokohama City University, International Graduate School of Arts and Sciences, Yokohama, Japan

The proteomic analysis of serum (plasma) has been a major approach to determining biomarkers essential for early disease diagnoses and drug discoveries. The determination of these biomarkers, however, is analytically challenging since the dynamic concentration range of serum proteins/peptides is extremely wide (more than 10 orders of magnitude). Thus, the reduction in sample complexity prior to proteomic analyses is essential, particularly in analyzing low-abundance protein biomarkers. Here, we demonstrate a novel approach to the proteomic analyses of human serum that uses an originally developed serum protein separation device and a sequentially linked 3-D-LC-MS/MS system. Our hollow-fiber-membrane-based serum pretreatment device can efficiently deplete high-molecular weight proteins and concentrate low-molecular weight proteins/peptides automatically within 1 h. Four independent analyses of healthy human sera pretreated using this unique device, followed by the 3-D-LC-MS/MS successfully produced 12 000–13 000 MS/MS spectra and hit around 1800 proteins (>95% reliability) and 2300 proteins (>80% reliability). We believe that the unique serum pretreatment device and proteomic analysis protocol reported here could be a powerful tool for searching physiological biomarkers by its high throughput (3.7 days per one sample analysis) and high performance of finding low abundant proteins from serum or plasma samples.

Received: October 27, 2005
Revised: April 26, 2006
Accepted: May 24, 2006

Keywords:
3-D-LC / Hollow-fiber membrane / Plasma / Serum

1 Introduction

A search for biomedically useful protein/peptide biomarkers has become a major goal in proteomic research with the recent progress in the mass spectrometric techniques for protein analysis. This is because, from the clinical viewpoint, the acquisition of effective biomarker information has emerged as an important issue. Once a useful biomarker (or a set of biomarkers) has been discovered, its measurement can be used to effectively predict the onset of a defined disease state, and its dynamic behavior could be an important hint for drug target discoveries [1–3]. Serum (or plasma) is the most valuable specimen for protein biomarker determination [4–8] because it is readily obtainable from a patient and contains thousands of protein species, which are secreted and produced from cells and tissues [9, 10]. Thus, the variation of protein components caused by diseases directly reflects the abundance of protein biomarkers in serum. However, the protein profile of serum is dominated by a handful of proteins present in high abun-

Correspondence: Dr. Giman Jung, Toray Industries, Inc., New Frontiers Research Laboratories, 1111 Tebiro, Kamakura, Kanagawa 248-8555, Japan
E-mail: Giman_Jung@nts.toray.co.jp
Fax: +81-467-32-8364

Abbreviations: HFMD, hollow-fiber-membrane based device; **HMW/LMW**, high/low-molecular weight (protein); **SCX**, strong cation exchange

dance, such as albumin, transferrin, haptoglobin, immunoglobulins and lipoproteins, which interfere with the identification of low-abundance protein biomarkers. Serum proteins are present in an extremely wide range of concentrations that are likely to extend by more than 10 orders of magnitude, and the 22 major protein species occupy approximately 99% of the total serum proteins ([4] and http://www.plasmaproteome.org). In human serum, it is estimated that up to 10 000 proteins are commonly present, most of which are present in relatively very low abundance [11]. Therefore, the reduction in the sample complexity (*e.g.*, to deplete high-abundance proteins and to replete low-abundance proteins) of serum samples is essential prior to any analyses aimed at determining proteins present in small quantities, which potentially include protein biomarkers.

There are two main methods of depleting these abundant proteins from serum samples. One is the affinity removal method, which uses antibody-based or affinity dye-based resins [12–21]. Currently, at least seven affinity removal columns or kits are commercially available for depleting 1–6 species of the major abundant serum proteins. One of the most successful devices for this approach is the Multiple Affinity Removal System (Agilent technologies), which is composed of bead-fixed antibodies against six major serum proteins, and can reduce these proteins to less than 1/1000-fold. Although the affinity removal method efficiently depletes several abundant serum proteins, the identification of low-abundance-protein biomarkers is still challenging because, even after the depletion, the remaining proteins (most of them have molecular weights higher than the serum albumin) are still sufficiently abundant to hamper the low-abundance protein biomarker determination.

The other method of reducing the level of abundant proteins from serum samples is the membrane removal method [22–27]. This method employs membrane filtration such that low-molecular weight (LMW) proteins are separated from high-molecular weight (HMW) ones. Many low-abundance serum proteins, including biomarkers, are classified as LMW proteins compared with serum albumin [28–30]. Such LMW proteins may be related to diseases, and reflect the state of cells and tissues [9, 10]. An approach to fractionate these LMW proteins in serum samples by centrifugal ultrafiltration followed by MS has been reported previously, and led to the successful concentration of LMW proteins and identification of 341 serum proteins [23].

In proteomic research, the performance of MS depends on sample conditions. In addition to the reduction in sample complexity (*i.e.*, depletion of abundant proteins), serum proteins must be free of salts, detergents and other contaminants, and the amount of proteins or peptide fragments injected into the mass spectrometer per defined time unit should be controlled. For these reasons, to increase the number of identified proteins in serum samples, additional procedures are required, which are generally time consuming, *i.e.*, sample cleanings or separations. Although various approaches have been developed for obtaining better conditions, *i.e.*, more proteins identified within a shorter time, the throughput and performance of proteomic research using human serum samples are still unsatisfactory.

Here we propose a novel approach that uses an originally developed abundant serum protein depletion device based on high-performance hollow-fiber membranes (HFM), and a 3-D LC system prior to MS. This unique protocol enabled us to collect almost 12 000–13 000 MS/MS spectra and hit around 1800 proteins (>95% reliability) and 2300 proteins (>80% reliability) within 3.7 days of analysis.

2 Materials and methods

2.1 Materials

Four standard human serum samples were prepared from 12 healthy volunteers, each sample comprising sera from 3 volunteers. The gels for SDS-PAGE and sequencing grade-modified trypsin were obtained from Invitrogen Corporation and Promega, respectively. Ammonium bicarbonate (NH_4HCO_3) was obtained from Sigma. HPLC-grade pure water, ACN and formic acid were purchased from Wako Pure Chemicals (Japan).

2.2 Depletion of HMW serum proteins using the HFM-based device

The serum was filtered through a 0.22-μm-pore-size filter. The initial protein concentration of the serum was determined by BCA protein assay (Pierce) and adjusted to 50 mg/mL. One milliliter of the serum sample was diluted to 12.5 mg proteins/mL by adding 3 mL 25 mM ammonium bicarbonate buffer (pH 8.0). Four milliliters of the serum dilution was injected into the HFM-based device (HFMD). After 1 h of operation, the solution with LMW serum proteins was recovered, and lyophilized or directly injected for RP chromatography. An aliquot of the resuspended sample was analyzed by SDS-PAGE using a 4–12% Bis-Tris gel. Bands were quantitated with ImageQuant software (GE healthcare). The concentrations of the HSA, β_2-microglobulin and α-fetoprotein were measured using ELISA Quantification kits in accordance with manufacturer's protocols (HSA, Bethyl Laboratories; β_2-microglobulin, Alpha Diagnostic International; α-fetoprotein, R&D Systems).

2.3 Depletion of high-abundance serum proteins by affinity method

An antibody-based column (Multiple Affinity Removal System, Agilent) was used for the affinity removal experiments. The serum sample (15 μL) was diluted with the buffer supplied with the kit. The column was used according to the manufacturer's protocol. An aliquot of the sample passed through the column was electrophoresed on gels together with the HFMD-treated serum.

